

Cost Optimization of US Sustainable Aviation Fuel Supply Chain Under Different Policy Constraints

by

Walter T. Kelso III

B.S.E. Aerospace Engineering, University of Michigan (2019)

Submitted to the Department of Aeronautics and Astronautics
in partial fulfillment of the requirements for the degree of

Master of Science in Aeronautics and Astronautics
at the
MASSACHUSETTS INSTITUTE OF TECHNOLOGY

September 2021

© Massachusetts Institute of Technology 2021. All rights reserved.

Author.....
Department of Aeronautics and Astronautics
August 6, 2021

Certified by.....
Steven R. H. Barrett
Professor of Aeronautics and Astronautics
Thesis Supervisor

Accepted by.....
Jonathan How
Professor of Aeronautics and Astronautics
Chair, Graduate Program Committee

Cost Optimization of US Sustainable Aviation Fuel Supply Chain Under Different Policy Constraints

by

Walter T. Kelso III

Submitted to the Department of Aeronautics and Astronautics
on August 6, 2021, in partial fulfillment of the
requirements for the degree of
Master of Science in Aeronautics and Astronautics

ABSTRACT

This thesis quantifies the costs and emissions of a potential sustainable aviation fuel supply chain in the US in 2035 while incorporating regional uncertainty analysis. Feedstock availability is quantified using projected arable land availability, agricultural yields, and projected waste and residue availability. A mixed-integer linear programming model was developed to minimize supply chain costs, subject to uncertain variables which were analyzed using Monte Carlo simulations. Under a baseline set of assumptions, an average of 78% of 2035 US jet fuel demand can be met with sustainable aviation fuels. The optimization model is applied using inputs from four socioeconomic scenarios to meet 25% and 50% of projected 2035 demand. The sensitivity of the results to a carbon emissions cost of 100 \$/tonne CO_{2e} is also evaluated. Under a baseline set of assumptions, when 50% of 2035 US demand is offset, sustainable aviation fuel is produced with 50% higher costs and 39% lower emissions than conventional jet fuel. In all scenarios, the introduction of a 100 \$/tonne CO_{2e} carbon emissions cost resulted in optimized supply chains using feedstocks and pathways with lower life cycle emissions but higher capital costs.

Thesis Supervisor: Steven R. H. Barrett

Title: Professor of Aeronautics and Astronautics

Acknowledgements

I would like to thank all of the following people for their support during my time at MIT.

My advisor, Professor Steven Barrett, for giving me the opportunity to research as a member of the Laboratory for Aviation and the Environment.

Dr. Ray Speth and Dr. Florian Allroggen, for directly supervising my research and providing critical advice and ideas.

Matthew Pearlson, for always finding time to meet and answer all of my questions.

All of the members of the LAE, for creating a fun and collaborative work environment.

My friends from the University of Michigan, especially Alex, Tim and Harry, for their conversations and jokes.

Finally, my Mom, Dad and sister Megan, for all of their unconditional love and support.

Contents

Chapter 1	Introduction.....	7
Chapter 2	Methods.....	9
2.1	Feedstock Availability	9
2.1.1	Energy Crops	11
2.1.2	Crop Residues	13
2.1.3	Forestry Residues.....	14
2.1.4	Waste fats, oils and greases (FOG).....	15
2.1.5	Municipal Solid Waste (MSW).....	16
2.2	GHG emissions modeling	17
2.2.1	Emissions Factors	17
2.2.2	Feedstock Production Emissions	18
2.2.3	Feedstock-to-fuel Conversion Emissions.....	19
2.2.4	Transportation Emissions.....	19
2.2.5	Land Use Change Emissions.....	20
2.3	Financial modeling.....	20
2.3.1	Utility Costs	20
2.3.2	Feedstock Production Costs.....	21
2.3.3	Refinery Financial Assumptions.....	22
2.3.4	Transportation Costs	23
2.3.5	Land Use Change Costs	23
2.4	Transportation Modeling.....	24
2.5	Jet Fuel Demand	24
2.6	Supply Chain Optimization.....	24
Chapter 3	Results.....	33
3.1	Potential SAF Production.....	33
3.2	Baseline Optimization Scenario Results	34
3.2.1	Carbon Pricing Sensitivity Results	34
3.2.2	Supply Chain Scaling Sensitivity Results	40
3.3	Alternative Scenario Results.....	42
Chapter 4	Conclusions.....	45
Appendix A	Pathway Inputs and Outputs	47
Appendix B	Additional Model Inputs	51
Appendix C	Additional Results.....	56

Chapter 1 Introduction

In 2019, commercial aviation accounted for approximately 2% of US greenhouse gas (GHG) emissions [1]. The environmental impact of aviation is expected to increase, as the North American commercial aviation market is expected to grow by approximately 3% annually from 2020-2039 [2]. Sustainable aviation fuels (SAF), with lower life cycle emissions than conventional jet fuel, have been identified as a short- to medium-term solution to mitigate commercial aviation's environmental impact [3]. These sustainable aviation fuels have been approved as drop-in fuels, which can be used in the engines of existing aircraft.

The life cycle emissions of SAF pathways have been studied extensively [4–7]. These studies found that, depending on the feedstocks and fuel conversion pathways considered, sustainable aviation fuels provide life-cycle GHG reductions of 26% to 91% from conventional jet fuel. The potential global emissions reduction from the use of alternative jet fuels in the year 2050 was evaluated in Staples et al. 2018 [8]. A similar study was conducted for the US for the year 2050 [9]. These studies found that the use of SAF could reduce 2050 worldwide aviation emissions by a maximum of 68%, and US aviation emissions by 42%. However, these life cycle assessment (LCA) studies and system wide analyses do not account for regional uncertainty, and treat uncertain variables such as crop yield and fuel conversion efficiency deterministically. Therefore, these deterministic studies do not quantify the range of potential GHG emissions reductions from a SAF supply chain that may occur from different realizations of uncertain variables. The production costs associated with SAF pathways have been quantified using techno-economic analysis (TEA) and determined to come at a cost premium to conventional jet fuel production costs [10,11]. However similar to previous LCA analyses, these TEA studies have not accounted for regional variability in key inputs such as capital area cost factors and utility costs.

Previous studies have built on LCA and TEA analyses to minimize US SAF supply chain costs or emissions using linear optimization models. Lewis et al 2018 use a geospatially explicit linear optimization model to produce a cost-minimized US nationwide SAF supply chain based on waste and

residue feedstock availability and demand centers [12]. Other studies have optimized SAF production using wastes and residues for a regional supply chain while minimizing costs or emissions and meeting various fuel demand levels [13,14]. However, no previous study has evaluated the costs and emissions of a US SAF supply chain using wastes, residues and crops while incorporating uncertainty analysis.

The objectives of this study are to quantify the potential production capacity of SAF in the US in 2035, and to evaluate the costs, emissions, abatement costs and feedstocks and pathways used in the optimal SAF supply chain, subject to uncertainty in pathway inputs and variations in scenario assumptions. In this analysis, we use a cost minimization spatially resolved linear programming model to quantify the costs and emissions associated with a three-stage SAF supply chain in the US in the year 2035 while incorporating regional uncertainty and variability in key inputs. The supply chain is also evaluated under variations in the fraction of total jet fuel demand fulfilled, cost of carbon emissions, and socioeconomic scenario projections. We evaluate the potential production of sustainable aviation fuel in the US in 2035 using crops, waste oils and greases, crop residues, forestry residues and municipal solid waste (MSW). The conversion of these feedstocks to jet fuel is considered using: Alcohol-to-Jet (ATJ) via ethanol, Hydroprocessed esters and fatty acids (HEFA), Synthesized iso-paraffins (SIP), and Fischer-Tropsch (FT) [15]. The supply chain costs and emissions associated with each feedstock and pathway are calculated using harmonized regional stochastic inputs. The SAF supply chain is then optimized using a mixed-integer linear programming model. This study is the first to evaluate a potential US sustainable aviation fuel supply chain using a linear optimization model while incorporating uncertain regional inputs.

Chapter 2 Methods

In this analysis, we first calculate 2035 SAF feedstock availability on the county level for 15 feedstocks. Next, we introduce the mass and energy balances and associated uncertainties in the six feedstock-to-fuel pathways under consideration. We quantify the costs and lifecycle emissions associated with feedstock production, transportation, fuel production and fuel transportation using regional data and uncertainty analysis. All costs and emissions are allocated among output products according to their energy output shares [16]. Airport level jet fuel demand is calculated and aggregated to the county level. Cost and emission inputs that are uncertain are simulated using Monte Carlo analysis. Following the Monte Carlo analysis, the uncertain inputs are used in a three-stage single period optimization model, which outputs the optimal minimum cost SAF supply chain for each run case, subject to demand requirements. The optimization model is also run with carbon emissions costs of 0 \$/tonne CO_{2e} and 100 \$/tonne CO_{2e} to evaluate the impact of carbon pricing on supply chain costs and emissions. The change in costs and GHG emissions compared to petroleum-derived jet fuel is assessed. A summary of the methods used in this analysis is presented in Figure 2-1.



Figure 2-1. Flow chart of analysis.

2.1 Feedstock Availability

Four main scenarios are considered in this analysis to evaluate future potential SAF supply chains. The key inputs for each of these scenarios are shown in Table 2-1. Scenario 1 is considered the baseline scenario in this analysis.

Table 2-1. Scenario Assumptions for 2035.

	Scenario 1	Scenario 2	Scenario 3	Scenario 4
Land Use Pattern under Special Report Emissions Scenarios	A1B	A2	B1	B2
Hadley climate change scenario for GAEZ yields	A1F1	A2	B1	B2
Shared Socioeconomic Pathways	SSP5	SSP3	SSP1	SSP2
2016 Billion Ton Report Wood Energy and Market Scenario	High Housing, High Wood Energy Demand	Moderate Housing, High Wood Energy Demand	High Housing, Low Wood Energy Demand	Moderate Housing, Low Wood Energy Demand
Agro-climatic suitability threshold	Moderate	Medium	Good	Medium
Pastureland availability	20%	10%	10%	10%

Ten cultivated energy crops, crop residues and forestry residues, waste fats, oils and greases (FOGs), and MSW are considered as feasible feedstocks for SAF. The conversion pathways considered for each feedstock are shown in Table 2-2. Although many of the feedstocks listed may be used in multiple pathways, each feedstock is mapped to only one pathway in this analysis. Crop availability and crop residue availability are treated as uncertain, while MSW, FOG and forestry residue availability is deterministic and scenario dependent.

Table 2-2. Feedstocks and pathways considered.

Feedstock	Pathway	Fuel Products	Source
Corn Grain Sorghum Wheat	ATJ	Jet, Gasoline, Diesel	[17,18]
Soybean Canola Sunflower	HEFA crop	Jet, Gasoline, Diesel, Lightends	[5,17,19]
Sugarcane Sugarbeet	SIP	Jet	[4,7]
Miscanthus Switchgrass Crop Residue Forestry Residue	FT biomass	Jet, Naphtha, Diesel	[20]
Used Cooking Oil Animal Fats	HEFA FOG	Jet, Gasoline, Diesel, Lightends	[5]
Municipal Solid Waste	FT MSW	Jet, Diesel, Gasoline	[21]

2.1.1 Energy Crops

Land use in the conterminous US in 2035 is estimated using data sets from the US Geological Survey (USGS) FORE-SCE model, which contains annual land use projections at a spatial resolution of 250 meters for four scenarios (A1B, A2, B1, B2) based on the Intergovernmental Panel on Climate Change (IPCC) Special Report on Emission Scenarios (SRES) [22]. Land is considered available for conversion to cropland for SAF production only if it is designated as grassland, shrubland, or pastureland. Between 10-20% of pastureland is available for conversion to crop land, as shown in Table 2-1, in order to preserve land for livestock grazing [8]. The available pastureland is then aggregated from the 250-meter resolution dataset to the county level.

The pastureland available for conversion to cropland for each crop in each county is further limited by imposing a minimum suitability condition using the Global Agro-ecological Zones (GAEZ) version 3.0 model developed by the International Institute for Applied Systems Analysis (IIASA) and the Food and Agriculture Organization of the United Nations (FAO) [23]. The GAEZ model calculates crop suitability

on a 5 arc-minute grid cell resolution by comparing crop-specific growth requirements to local climate and soil conditions at various agricultural input levels and time frames. In this analysis, we assume high input levels and rainfed systems, to avoid diverting water resources from food crops or human use. Additionally, GAEZ models the mean suitability for three 30-year periods: 2011-2040, 2041-2070, and 2071-2100. We use data for 2011-2040 and consider three suitability levels, “moderate”, “medium”, and “high”. Land below the minimum crop-specific suitability level is not considered available for conversion, in order to limit converting land where crop cultivation is unlikely.

Ten crops are considered as feedstock for SAF: corn, sorghum, wheat, soybean, canola, sunflower, sugarcane, sugarbeet, miscanthus and switchgrass. Multi-cropping is not considered in this analysis therefore if land is converted from pastureland to cropland, only one crop is considered for cultivation annually. Eight of these ten crops are historically grown in the US, with the exceptions being the energy grasses miscanthus and switchgrass. For these eight crops, US Department of Agriculture (USDA) county-level yield data is extrapolated to 2035 with a 95% confidence interval, which is used to construct triangular distributions for uncertainty analysis [24]. In counties in which historical yield data is insufficient, state level data is used. Switchgrass and miscanthus yields are taken from the 2016 Billion-Ton Report [25], in which data from over 110 field trials was used to estimate county-specific per-acre yields based on 30-year historic weather data for switchgrass and miscanthus. In this analysis, we use the base-case scenario from the BTR, which assumed a 1% annual yield improvement for energy crops through a 2015-2040 simulation period. To construct probability distributions for switchgrass and miscanthus, current yields are used as a lower bound, while a 2% annual yield improvement is assumed for the upper bound.

The GAEZ model is then used to impose an upper bound on the maximum attainable crop yields in each US state, under the assumed high input level and rainfed conditions. If the county-level crop yield extrapolated from historical USDA data exceeds the state-level GAEZ maximum attainable crop-yield, the GAEZ yield replaces the extrapolated yield in the triangular probability distribution. An example of

this method is shown in Figure 2-2, in which historical county level corn yield data from Jasper County, Indiana is linearly extrapolated to 2035 with a 95% confidence interval. In this example, the upper estimate for corn yield in 2035 exceeds the GAEZ maximum attainable yield in Indiana, so the GAEZ yield is used as the upper bound in a triangular probability distribution for 2035 corn yield in Jasper County, Indiana.

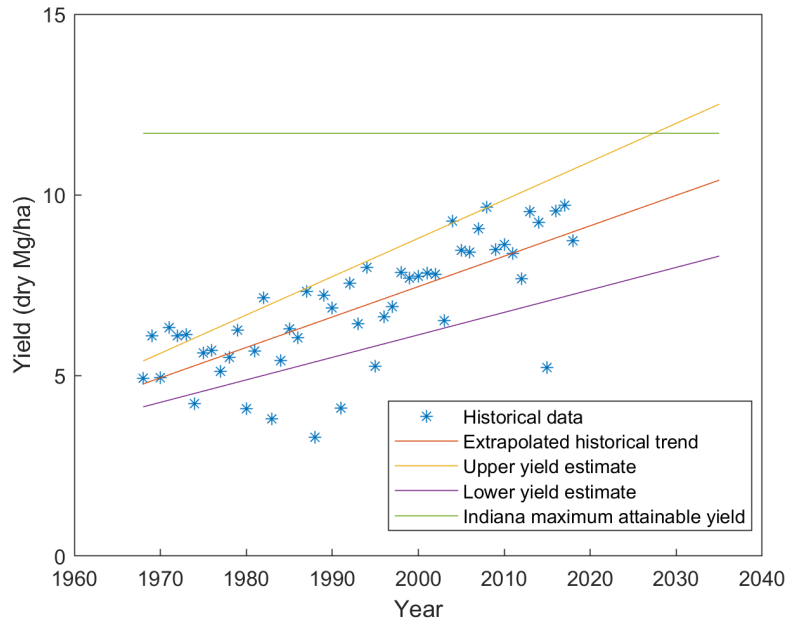


Figure 2-2. Yield Extrapolation of corn yields in Jasper County, Indiana.

2.1.2 Crop Residues

The production of crop residue is considered for the eight annual crops previously mentioned. The annual per-acre yield of each of these crops is extrapolated to 2035. However, since these crops are grown on cropland, the maximum attainable yield data from irrigated land, rather than from rainfed land, is used from the GAEZ model to provide an upper bound. Crop residue production is estimated by multiplying per-acre yields by the crop-specific straw-to-grain ratio shown in Table 2-3 [26].

Table 2-3. Crop-specific straw to grain ratios.

Crop	Straw/grain ratio
Corn	1.0
Sorghum	1.5
Wheat	1.5
Soybean	1.0
Canola	1.5
Sunflower	1.0
Sugarcane	0.25
Sugarbeet	0.25

The mix of crops grown in each county on cropland is calculated using data from the 2019 USDA Cropland Data Layer (CDL) [27]. The CDL is a 30-meter resolution crop-specific land cover data layer created annually for the continental US using satellite imagery and agricultural ground truth. The county specific cropland distribution of crops is assumed to stay constant through 2035. Cropland area projections are estimated using the FORE-SCE model, and aggregated to the county level. The county-level sustainable residue removal rates, defined as the fraction of crop residue that can be removed without causing erosion or soil organic carbon loss, for corn, wheat and sorghum are taken from Muth et al. 2013 [28], and compared to county-level yield data from the USDA. The average sustainable residue removal rate for corn, wheat and sorghum in each county is used as the sustainable residue removal rate for the other five annual crops considered in this analysis. For reference, the average sustainable residue removal rate for corn across all counties in the US is 31%, with a standard deviation of 22%. The total crop residue produced in each county is therefore a function of cropland area, crop mix, irrigated crop yields, straw to grain ratios, and sustainable residue removal rates. The total amount of crop residue varies in each Monte-Carlo run case due to crop yield uncertainties.

2.1.3 Forestry Residues

County level forestry residue availability in 2035 is taken from the 2016 Billion Ton Report (BTR) [25]. The BTR uses a linear programming model to estimate forestland production over time. The model

accounts for various logging methods, forest stand species, and location specific logging residue retention rates and aggregates results to the county level. Additionally, the BTR analyzed six potential future scenarios, with three levels of demand for biomass for energy, and three levels of demand for housing. The scenarios we used in this analysis are shown in Table 2-1. We note that similar to our analysis, the BTR assumes there is no land use change from/to forestry and non-forestry use.

2.1.4 Waste fats, oils and greases (FOG)

The production of yellow grease and rendered animal fats are estimated on a per capita basis. County level population projections for all US counties in the year 2035 are taken from Hauer 2019 [29]. Hauer projects the US population in five-year intervals for the period 2020-2100 controlled to the five Shared Socioeconomic Pathways (SSPs). The SSPs are mapped to the scenarios in our analysis as shown in Table 2-1.

Yellow grease production is estimated as 4 kg per person per year [30], with a collection rate of 85% based on USDA data [31]. Based on current yellow grease utilization in the United States, we further assume that 13% of yellow grease is used for animal feed, 30% is used for biodiesel, with the remainder available for SAF production [30].

We analyze rendered animal fat generation for poultry, cattle and pigs. The USDA projects that per capita meat consumption in the US will increase from 2019 to 2029 by less than 1%, therefore we assume that per capita livestock slaughter will remain constant to 2035 [32]. Per capita livestock production is shown in Table 2-4. County-level animal production is estimated using future population projections and county level livestock inventory from the 2017 USDA Census of Agriculture [33]. The spatial distribution of livestock is assumed constant to 2035.

Table 2-4. Per capita liveweight livestock production in the US in 2035.

Product	Per Capita Production (kg/year)
Cattle	60.5
Pigs	47.7
Poultry	88.5

We use the method from Milbrandt et al. 2018 [30] to calculate the availability of rendered animal fats for the SAF industry. The fat percentage of the liveweight of each animal is applied, and the edible fat percentage is subtracted. Additionally, a large fraction of rendered animal fats is currently used in the animal feed industry and for biodiesel production. The key inputs for calculating rendered animal fat availability for the SAF market is shown in Table 2-5.

Table 2-5. Waste FOG assumptions [30].

	Fat % of liveweight	Inedible fat % of total fat	% of inedible fat not used in other industries	Net waste FOG available from animal liveweight
Cattle	12%	64%	28%	2.2%
Pigs	5%	89%	20%	0.9%
Poultry	3%	100%	37%	1.1%

2.1.5 Municipal Solid Waste (MSW)

MSW production is calculated on a per capita basis and projected to the year 2025 [34]. The 2025 projections show a less than one percent change from current empirical data, therefore annual per capita MSW production of 840 kg is assumed constant to 2035. County-level MSW availability is calculated by combining county-level population projections with per capita MSW production. The composition of MSW is assumed constant to 2035, and is provided for 2014 by the Environmental Protection Agency (EPA), as is landfill rate by component, and is shown in Table 2-6 [35]. The system boundary of the MSW Fischer-Tropsch (FT) pathway is set where MSW discards exit a sorting facility as described in

Suresh et. al 2018 [21], therefore only the MSW that remains after recycling and compost enter this analysis.

Table 2-6. MSW composition and landfill rate.

Material	Share of each component	Component landfill rate
Paper	26.6%	28.4%
Organics	34.4%	57.4%
Plastics	12.9%	75.5%
Metals and Glass	13.4%	57.2%
Rubbers, leather, textiles	9.5%	59.8%
Other	3.2%	58.1%

2.2 GHG emissions modeling

GHG emissions are modeled along each step of the SAF supply chain: land use conversion, feedstock cultivation, feedstock conversion to SAF, feedstock and fuel transportation, and fuel combustion.

2.2.1 Emissions Factors

The emissions factors of electricity and hydrogen are projected to change in the future due to the increased use of production methods with lower life cycle emissions. These changes will impact the total life cycle emissions of the SAF supply chain [8]. The emissions factors for other energy inputs such as natural gas are assumed constant to 2035 and are taken from the GREET 2020 model. Electricity emissions factors are projected annually for the period 2019-2050 by the Energy Information Administration for the nine US Census Divisions [36]. In this analysis we use the 2035 reference case, which projects a 25% reduction in the average US electricity emissions factor from 2019. The electricity emissions factor for each US Census Division is shown in Table B-1 in Appendix B .

The emission factor for US hydrogen in 2035 is based on projections from Singh et. al 2005 and the 2006 World Energy Outlook [37,38]. Three hydrogen production source mixes are considered and are based on the current production method modeled in GREET, and the “reference” and “carbon constraint” cases for

North America in the year 2030 from the World Energy Outlook. We use the current hydrogen emissions factor when modeling Scenario 1, the 2035 “reference” case when modeling Scenarios 2 and 4, and the “carbon constraint” case when modeling Scenario 3. Singh et al. project that hydrogen produced by renewables will come from 70% biomass, 26% wind and 4% solar. The emissions factors for the reference and carbon constraint cases were calculated by modeling the projected mixes in GREET. The hydrogen production methods and corresponding emissions factors are shown in Table B-2 in Appendix B .

2.2.2 Feedstock Production Emissions

Data availability determines the resolution of emissions modeling for each feedstock. Cultivated crop production emissions are modeled on the state level. Waste grease rendering emissions are modeled on a regional level, while forest residue emissions and crop residue production emissions are modeled on a national level.

Crop yield projections for 2035 are determined on a county level using the method described in Section 2.1.1. State level nitrogen, phosphate and potash fertilizer application rates for corn, wheat and soybean from 1964-2018 are taken from the USDA, and extrapolated to 2035 [39]. For all other crops, state level crop enterprise budgets are used to obtain current fertilizer application rates. A list of enterprise budgets used in this analysis is provided in Table B-3 in Appendix B . The average increase in application rate for corn, wheat and soybean is obtained for each state and fertilizer, and is used to estimate the future application rates for the other seven crops. Herbicide and pesticide application rates for all crops are obtained from state level enterprise budgets [8]. Farming energy requirements are treated as uncertain, and these probability distributions are shown in Table B-4 in Appendix B along with the breakdown of energy inputs for each crop. Farming energy requirements are assumed constant to 2035, and due to a lack of available data, are assumed constant throughout the US. Energy requirements for the production of forestry residues and crop residues are also assumed constant throughout the US and are shown in Table B-4. We assume that utilities are supplied by the state in which each county is located.

Crop residue production emissions are calculated using cultivation energy distributions and crop-specific nutrient replacement rates. The mass concentration of Nitrogen, Phosphorous and Potassium for residues of the eight annual crops considered in this analysis are taken from Chatterjee 2013 [40]. We assume complete replacement of the nutrients removed by crop residue harvesting.

The system boundary for HEFA fuels derived from yellow grease and animal fats begins with the rendering process. This follows the approach used in CORSIA and Seber et al 2014 [5,7]. Energy inputs for rendering yellow grease and animal fats are treated as uncertain, and probability distributions are derived from data from previous studies [5,41,42]. These rendering energy inputs are shown in Table B-5. Due to regional variations in electricity emissions factors, the emissions associated with the rendering step varies between US Census Divisions.

The system boundary of the MSW FT pathway is described in detail in Suresh et al 2018 [21]. Notably, the MSW system boundary excludes curbside collection, transportation and initial sorting, which must occur regardless. Additionally, we use the same parameter distributions for lifecycle emission Monte Carlo analysis as Suresh et al 2018.

2.2.3 Feedstock-to-fuel Conversion Emissions

In this study we model six alternative jet fuel pathways: ATJ, HEFA FOG, HEFA crop, SIP, FT biomass and FT MSW. Output fuel yields are modeled as probability distributions due to uncertainty in each pathway. These distributions along with detailed technical assumptions used for the mass and energy balances for each feedstock and pathway are found in Appendix A . We consider the “maximum jet” product profile from Pearlson et al 2013 for the HEFA pathway [11].

2.2.4 Transportation Emissions

We assume that feedstocks can be transported from supply counties to biorefinery counties via rail, trucking, and barge, while jet fuel is transported from refineries to airports via rail, trucking, barge and pipeline. The energy required to transport products on a per ton-mile basis is modeled in GREET for each

transportation mode. Transportation energy efficiency improvements from 2020 to 2035 are projected by the EIA and applied to the values from GREET [36]. The energy efficiency improvements for rail, freight trucking and domestic shipping are 9.4%, 17.8% and 9.4% respectively. GREET assumes that electricity is consumed to operate liquid pipelines, therefore the emissions associated with transportation of jet fuel via pipeline are reduced with lower future electricity emissions factors.

2.2.5 Land Use Change Emissions

GHG emissions as a result of changes in soil and biomass content are estimated using the Agro-ecological Zone Emission Factor (AEZ-EF) model, version 52 [43]. This model reflects the pulse of GHG emissions per unit area from a one-time change in land use, from pastureland to cropland with annual crop cultivation, miscanthus cultivation or switchgrass cultivation. We calculate the average LUC emissions factor in each county for each of these three land conversion pairings. LUC emissions are allocated using the energy allocation method, and are amortized over a 30-year period.

2.3 Financial modeling

Similar to GHG emissions, costs are modeled along each step of the SAF supply chain. All costs in this analysis are expressed in 2019 USD.

2.3.1 Utility Costs

US average electricity, natural gas and crude oil prices are projected to 2035 by the EIA [36]. We assume that these prices are uncertain, and use the EIA baseline, high economic growth and low economic growth cases to construct probability distributions, shown in Table B-6. We correlate historical state electricity and natural gas prices from 1990-2018 to the US average values, and use the 2035 US EIA projections to project 2035 state level electricity and natural gas prices in each Monte Carlo run case [44,45]. We also correlate historical crude oil prices to gasoline prices in each of the Petroleum Administration for Defense Districts (PADD) [46], which are then correlated to diesel and propane prices in each PADD region. These price correlations are shown in Table B-7.

Hydrogen production costs are dependent on the production mix assumed in 2035 as described in Section 2.2.1. Hydrogen production costs from wind and solar are taken from projections from IRENA 2019, and production costs from biomass and natural gas are from Parkinson et al 2019 [47,48]. The production costs and production mixes for each scenario are used to calculate the average hydrogen production cost. These production costs are shown in Table B-2 in Appendix B for each scenario. Other pathway input costs that are treated as deterministic and constant throughout the US are shown in Table B-8.

2.3.2 Feedstock Production Costs

Crop production costs are modeled on the county level, due to per acre fixed costs such as machinery capital recovery, and county level yields. State level crop-specific enterprise budgets are used to estimate per-acre crop production costs. These crop budgets include costs from: seed, fertilizer, herbicides and pesticides, fuel, lube and electricity, repairs, labor, land, custom services, machinery capital recovery, taxes and insurance, and farm overhead [49]. We use average costs from each USDA Farm Resource Region for states without crop-specific enterprise budgets.

Crop residue cultivation costs are also modeled on the county level due to fixed per acre costs and county-specific crop yields and sustainable residue removal rates. We model crop residue production costs from chopping, baling, on-farm hauling, and nutrient replacement. We use the assumptions from Gallagher et al 2003, which used the same chopping, baling and on-farm hauling costs for crop residue cultivation for all counties and crops [50]. Chopping, baling and on-farm hauling costs are taken from the 2020 Iowa Farm custom rate survey and are estimated as 12.40 \$/acre, 12.35 \$/bale and 3.15 \$/bale respectively [51]. We assume that one bale is equal to 1,200 pounds of dry crop residue [51].

Forest residue production costs are estimated using data from the Billion Ton Report. Logging residue harvesting costs for six forest stand types are modeled in five US regions assuming both clear cutting and thinning operations. The mix of stand type and cut option are unique to each county in each of the four future scenarios considered in our analysis. The harvesting costs range from 14.06 to 18.44 \$ per dry ton of logging residue [25].

Due to a lack of publicly available data, we do not estimate rendering costs for yellow grease and animal fats [31]. Instead, we use the market value of these products in this analysis to estimate production costs. Due to significant historical variability in the market prices of rendered animal fats and yellow grease, we treat these prices as uncertain and generate probability distributions based on historical data [52,53]. These probability distributions are shown in Table B-5. We assume FOG prices are uniform across the US in each Monte Carlo run case. We use the assumption from previous studies of zero-cost MSW feedstock [10,21].

2.3.3 Refinery Financial Assumptions

Biorefinery reference capacities and capital cost estimates are obtained from literature and shown in Table B-9. Capital cost estimates are adjusted to 2019 USD using the Chemical Engineering Plant Cost Index [54]. In the optimization analysis, we explore economies of scale by allowing potential refinery capacities to range from 1,000 to 10,000 barrels per day (BPD) of fuel products. A scaling factor of 0.7 is used for all biorefineries [55], while a scaling factor of 0.34 is used for crop oil production facilities [56]. The HEFA crop pathway requires both an oil extraction facility and a HEFA facility, which we assume are collocated in our optimization model. A piecewise linear approximation is applied to linearize the capital cost curves for use in the optimization model. The annual capital cost of each refinery is assumed to be 13.8% of capital investment costs and is calculated using a 20-year refinery lifetime and a weighted average cost of capital (WACC) of 12.5%, which is the average WACC of four public biofuel companies: Gevo, Aemetis, Renewable Energy Group and Alto Ingredients [57].

Based on the work of Bann et al. 2017, a beta PERT distribution that varies between 80% and 150% of the deterministic value was used to model uncertainty in capital cost estimates. Working capital is 5% of the fixed capital investment, and direct operating costs such as maintenance and overhead are 7.7% of the fixed capital investment [10]. We incorporate income tax by using the combined state and federal corporate income tax rates, and assume straight line depreciation for a 20-year refinery operating lifetime [58]. We account for location dependent cost differences in labor, equipment and materials by applying

county level area cost factors generated by the US Department of Defense [59]. Each refinery is assumed to operate for 350 days per year. Variable operating costs are calculated for each pathway using the inputs in Appendix A and costs in Appendix B .

2.3.4 Transportation Costs

Transportation costs per ton-mile via road, rail and barge are taken from the Bureau of Transportation Statistics [60]. We assume transportation costs are constant for all biomass on a total weight basis, and the cost of transporting all liquids is constant on a volumetric basis, following the assumptions in Parker et al 2010 [14]. Pipeline tariff rates for transport of jet fuel are route dependent and are modeled in the Freight and Fuel Transportation Optimization Tool (FTOT) [61]. We also use a transloading cost from FTOT to account for costs associated with switching transport modes. Transloading costs and road, rail and barge transportation costs for solids and liquids are shown in Table B-10.

2.3.5 Land Use Change Costs

Land conversion costs are separated into land establishment costs and vegetation clearing costs in accordance with the assumptions used in the Model of Agricultural Production and its Impact on the Environment (MAGPIE) [62]. MAGPIE is a global land use allocation model which calculates costs for the conversion of one land type to another. MAGPIE assumes a global establishment cost factor of 8000 \$/hectare, which is based on Kreidenweis et al 2018 [63]. The establishment cost accounts for the need for infrastructure and field preparation such as building farm roads, fencing, levelling and draining. MAGPIE also assumes a global clearing cost of 5 \$/tonne of carbon stock reduction in the soil. We use the land use change emissions data from the AEZ-EF model to calculate the land conversion cost for each AEZ and LUC pairing, while accounting for establishment and clearing costs. LUC costs are then amortized over a 30-year period.

2.4 Transportation Modeling

The transportation network from FTOT is used to model the distances and modes of transporting feedstock and jet fuel between counties. FTOT is a geospatially explicit model that uses a GIS-based multimodal network consisting of road, rail, water and pipeline networks in the US. FTOT also models intermodal facilities where mode transfers occur, and models tariff and capacity information for fuel product pipelines [61]. We use a shortest path algorithm, the modal transportation costs in Table B-10 and the network model from FTOT to determine the lowest cost routes for all possible origin and destination pairs of counties. We run this algorithm with the pipeline mode enabled when modeling jet fuel transportation, and disabled when modeling feedstock transportation. For transportation within a county, we assume road transport over a distance of two-thirds of the county radius, which is calculated using the county area [13].

2.5 Jet Fuel Demand

Future US jet fuel demand is modeled on an airport level and is constant in the four scenarios in this analysis. Commercial passenger flight traffic schedules from 2019 are taken from data from OAG, and separated into route-aircraft combinations [64]. We simulate fuel burn for each aircraft-route combination using the Aviation Emissions Inventory Code [65], and assume a 1% annual improvement in fuel burn across all aircraft-route combinations [66]. We project 2035 air traffic using the 2020 Boeing Commercial Market Outlook [2], which projects annual traffic growth by global region. We then calculate fuel burn totals by departure airport for the year 2035, and aggregate jet fuel demand to the county level. The total projected 2035 US jet fuel demand for scheduled passenger flights is 26.2 Billion gallons or 3.4 EJ.

2.6 Supply Chain Optimization

The objective of the optimization model is to minimize annual SAF supply chain costs that are composed of six costs: land use change costs (C_L), feedstock production costs (C_F), feedstock transportation costs (C_{TF}), refinery related costs (C_R), jet transportation costs (C_{TJ}), and jet combustion related costs (C_C) (Eq.

(1)). This model is similar to the renewable jet fuel supply chain model presented in Huang et al. 2019 [13].

$$\text{Minimize } C_L + C_F + C_{TF} + C_R + C_{TJ} + C_C \quad (1)$$

The inputs and decision variables used in this model are shown in Table 2-7 and Table 2-8 respectively.

Table 2-7. Inputs used in the optimization model.

Symbol	Description
P_i	Pastureland available for conversion to cropland in county i
S_{ni}	Pastureland available for conversion to cropland assuming feedstock n in county i
b_{ni}	Availability of feedstock n in county i (known for residues, FOG and MSW)
α_n^f	Allocation factor for feedstock n
α_r^p	Allocation factor for pathway r
c_{ni}^l	Unit annual land use change cost in county i assuming feedstock n
c_{ni}^f	Unit production cost of feedstock n in county i
c_{nij}^{tf}	Unit transportation cost for feedstock n from county i to county j
c_{nj}^r	Unit refinery variable operating cost for feedstock n in county j
c_{jk}^{ta}	Unit transportation cost of jet fuel from county j to county k
e_{ni}^l	Unit annual land use change emissions in county i assuming feedstock n
e_{ni}^f	Unit production emissions of feedstock n in county i
e_{nij}^{tf}	Unit transportation emissions for feedstock n from county i to county j
e_{nj}^r	Unit refinery related emissions for feedstock n in county j
e_{jk}^{ta}	Unit transportation emissions of jet fuel from county j to county k
e^c	Unit combustion emissions of jet fuel produced by the FT MSW pathway
q	Carbon cost
y_{ni}	Per acre crop yield of crop n in county i
λ_l^l	Minimum capacity limit of a refinery at capacity level l
λ_l^u	Maximum capacity limit of a refinery at capacity level l
β_n	Feedstock to fuel conversion efficiency for feedstock n
γ_n	Feedstock to jet conversion efficiency for feedstock n
D_k	Jet fuel demand in county k
A_j	Capital cost area cost factor in county j
x_{rl}	Fixed capital cost for a refinery at capacity level l for pathway r
z_{rl}	Variable capital cost for a refinery at capacity level l for pathway r
a	Annual refinery cost factor

Table 2-8. Decision variables in the optimization model.

Symbol	Description
l_{ni}	Pastureland converted to cropland for feedstock n in county i
t_{nij}^f	Amount of feedstock n transported from county i to county j
t_{nij}^a	Amount of SAF transported from county j to county k
R_{jrl}^f	Biorefinery fuel capacity in county j at level l with pathway r
R_{jr}^f	Total biorefinery fuel capacity in county j with pathway r
R_{jr}^a	Total biorefinery jet capacity in county j with pathway r
v_{jrl}	Binary variable indicating if there is a biorefinery in county j at level l using pathway r
v_{jr}	Binary variable indicating if there is a biorefinery in county j using pathway r
b_{ni}	Availability of feedstock n in county i (unknown for crop feedstocks)

The total amount of land converted in each county must be less than the available pastureland in that county (Eq. (2)). Additionally, since soil suitability requirements are unique to each crop and further limit land availability, the land converted for the purpose of cultivating each crop must be less than the crop-specific pastureland available in each county (Eq. (3)). The land use change costs (C_L) are allocated to jet fuel by the feedstock specific energy allocation factor α_n^f . The land use change costs are also a function of the land converted to cropland for each crop, the county and crop specific land use change costs and emissions, and the cost of carbon (Eq. (4)).

$$\sum_{n=1:10} l_{ni} \leq P_i \quad (2)$$

$$l_{ni} \leq S_{ni} \quad (3)$$

$$C_L = \sum_i \sum_{n=1:10} l_{ni} \alpha_n^f (c_{ni}^l + e_{ni}^l * q) \quad (4)$$

The feedstocks are numbered according to the order presented in Table 2-2, where feedstocks 1-10 represent the cultivated energy crops. The availability of energy crop feedstocks in each county is dependent on the land converted for those crops and their county specific yields (Eq. (5)). The availability of the waste and residue feedstocks are scenario specific and are assumed as inputs to the optimization model. The amount of each feedstock transported from supply counties to refinery counties must be less than the availability of each feedstock in the supply counties (Eq. (6)). The total feedstock production cost (C_F) is then a function of the total amount of each feedstock transported, feedstock energy allocation factors, unit feedstock production costs, unit feedstock production emissions and the cost of carbon (Eq. (7)).

$$b_{ni} = l_{ni}y_{ni}, \quad \forall n = 1:10 \quad (5)$$

$$t_{nij}^f \leq b_{ni} \quad (6)$$

$$C_F = \sum_n \sum_i \sum_j t_{nij}^f \alpha_n^f (c_{ni}^f + e_{ni}^f q) \quad (7)$$

The total feedstock transportation cost (C_{TF}) is a function of the total amount of each feedstock transported, feedstock allocation factors, the costs and emissions associated with transporting each feedstock from supply counties to refinery counties, and the cost of carbon (Eq. (8)).

$$C_{TF} = \sum_n \sum_i \sum_j t_{nij}^f \alpha_n^f (c_{nij}^{tf} + e_{nij}^{tf} q) \quad (8)$$

The model uses a piecewise linear approximation to estimate capital investment costs for each type of refinery at three capacity levels: 1,000-4,000 BPD, 4,000-7,000 BPD, and 7,000-10,000 BPD. If a refinery using pathway r exists in county j at capacity level l , the total fuel capacity must be between the minimum and maximum capacities for that level (Eq. (9)). The feasible feedstock and pathway combinations assumed in this analysis are shown in Table 2-2. We assume that only one refinery of each pathway may exist in each county (Eq. (10)), and therefore the sum of refinery capacities at all levels for pathway r in county j must equal the total capacity for that pathway and county (Eq. (11)). The total fuel produced at a refinery using pathway r is equal to the sum of compatible feedstocks transported to that county and the feedstock specific feedstock-to-fuel conversion efficiency (Eq. (12)-(17)). We assume that in each optimization run case, the fuel conversion efficiency for each pathway is uniform for all potential refineries. The total fuel capacity is used, as opposed to the jet capacity, because reference capital costs and capacities from previous studies are expressed in terms of total fuel capacity. Additionally, this allows the capacity levels to remain uniform between pathways even though the output product slate is unique to each pathway.

$$\lambda_l^l v_{jrl} \leq R_{jrl}^f \leq \lambda_l^u v_{jrl} \quad (9)$$

$$\sum_l v_{jrl} = v_{jr} \quad (10)$$

$$\sum_l R_{jrl}^f = R_{jr}^f \quad (11)$$

$$\sum_{n=1:3} \sum_i t_{nij}^f \beta_n = R_{j1}^f \quad (12)$$

$$\sum_{n=4:6} \sum_i t_{nij}^f \beta_n = R_{j2}^f \quad (13)$$

$$\sum_{n=7:8} \sum_i t_{nij}^f \beta_n = R_{j3}^f \quad (14)$$

$$\sum_{n=9:12} \sum_i t_{nij}^f \beta_n = R_{j4}^f \quad (15)$$

$$\sum_{n=13:14} \sum_i t_{nij}^f \beta_n = R_{j5}^f \quad (16)$$

$$\sum_{n=15} \sum_i t_{nij}^f \beta_n = R_{j6}^f \quad (17)$$

The total jet fuel produced at a refinery using pathway r is equal to the sum of compatible feedstocks transported to that county and the feedstock specific feedstock-to-jet conversion efficiency (Eq. (18)-(23)). The jet fuel transported from each county must be equal to the amount of jet fuel produced by each refinery in that county (Eq. (24)). Additionally, the total amount of jet fuel transported to each county k must meet or exceed the demand (Eq. (25)).

$$\sum_{n=1:3} \sum_i t_{nij}^f \gamma_n = R_{j1}^a \quad (18)$$

$$\sum_{n=4:6} \sum_i t_{nij}^f \gamma_n = R_{j2}^a \quad (19)$$

$$\sum_{n=7:8} \sum_i t_{nij}^f \gamma_n = R_{j3}^a \quad (20)$$

$$\sum_{n=9:12} \sum_i t_{nij}^f \gamma_n = R_{j4}^a \quad (21)$$

$$\sum_{n=13:14} \sum_i t_{nij}^f \gamma_n = R_{j5}^a \quad (22)$$

$$\sum_{n=15} \sum_i t_{nij}^f \gamma_n = R_{j6}^a \quad (23)$$

$$\sum_k t_{jk}^a = \sum_r R_{jr}^a \quad (24)$$

$$\sum_j t_{jk}^a \geq D_k \quad (25)$$

The annual refinery related costs (C_R) are a function of operating costs and annual capital related costs (Eq. (26)). The operating costs are a function of the total amount of feedstock transported to county j , feedstock allocation factors, the cost and emissions associated with converting one unit of feedstock to jet fuel, and the cost of carbon (Eq. (27)). Annual refinery capital costs are linearly related to refinery capital investment costs by the input a , which is the sum of the annual annuity factor (13.8%), working capital (5%) and direct operating cost (7.7%) assumptions. Refinery capital investment costs at each capacity level are the sum of fixed and variable capital related costs which are a result of the piecewise linear approximation to the capital cost curve. Annual capital related costs are also a function of the county-

specific area cost factor, and the pathway specific allocation factor, which is the average allocation factor of the feedstocks used by each pathway (Eq. (28)).

$$C_R = O + I \quad (26)$$

$$O = \sum_j \sum_i \sum_n t_{nij}^f \alpha_n^f (c_{nj}^r + e_{nj}^r q) \quad (27)$$

$$I = \sum_r \sum_j \sum_l \alpha_r^p A_j (x_{rl} v_{jrl} + R_{jrl}^f z_{rl}) a \quad (28)$$

The jet transportation cost (C_{TJ}) is a function of the amount of jet fuel transported, the costs and emissions associated with transporting jet fuel from refinery counties to demand counties, and the cost of carbon (Eq. (29)).

$$C_{TJ} = \sum_j \sum_k t_{jk}^a (c_{jk}^{ta} + e_{jk}^{ta} q) \quad (29)$$

The jet combustion cost (C_C) is a result of non-biogenic combustion emissions due to jet fuel produced via the FT MSW pathway. A portion of the carbon in MSW is non-biogenic, therefore a percentage of combustion emissions from FT MSW SAF must be considered in this analysis. The non-biogenic proportion of carbon in MSW is treated as stochastic and the associated probability distribution is taken from Suresh et al. 2018 [21]. The jet combustion cost is a function of the total MSW transported to refineries, the feedstock-to-jet conversion efficiency, the emissions associated with the combustion of the non-biogenic portion of MSW derived jet fuel, and the cost of carbon (Eq. (30)).

$$C_c = \sum_i \sum_j t_{nij}^f \gamma_n e^c q, \quad n = 15 \quad (30)$$

To reduce the overall problem size, we restrict feedstock transportation to routes in which the unit feedstock transportation cost is below 50 \$/short ton. This corresponds to a maximum transportation distance of 240 miles if the feedstock is transported only via trucks. This is in line with the ethanol industry, where most ethanol plants in the US are located within 50 miles of feedstock-producing areas [67]. We do not restrict jet fuel transportation.

The uncertain inputs described in previous sections are modeled stochastically using a Monte Carlo simulation in MATLAB. The MATLAB model was run 100 times for each of the four scenarios considered and sampled values from each probability distribution, which provided the input values necessary for the supply chain optimization. The optimization model was then run to meet 50% and 25% of demand in Scenario 1, and 25% of demand in Scenarios 2-4. Additionally, for each of these scenarios and demand levels, a carbon emissions cost of 0 \$/tonne CO_{2e} and 100 \$/tonne CO_{2e} are evaluated. This results in a total of 1,000 optimization model runs. The model is developed in the Julia language version 1.0.5 and solved using Gurobi 9.1.1 with the optimality gap set at 3%.

Chapter 3 Results

3.1 Potential SAF Production

We first assess the feasibility of meeting 2035 US jet fuel demand by calculating the maximum potential SAF production in 100 run cases of each of the four scenarios. In each run case, we assume all available residues and waste products are converted to jet fuel, and all available pastureland meeting crop suitability conditions in each county is converted to cropland. We assume the crop yielding the most jet fuel in each county is cultivated for this part of the analysis. The mean and 95% confidence intervals of SAF production potential from 100 runs of each of the four scenarios considered are shown in Table 3-1.

Table 3-1. Mean and 95% confidence interval of potential SAF production.

Scenario	Potential SAF Production (Billion Gallons)
S1	20.35 [18.37-23.19]
S2	10.78 [9.43-12.35]
S3	9.42 [8.18-10.74]
S4	10.40 [9.15-11.81]

Considering the projected 2035 US jet fuel demand is 26.2 billion gallons, it is not feasible to meet all of US jet fuel demand with SAF under the set of assumptions considered in this analysis. Scenario 1 produces the most SAF due to the 20% pastureland availability assumption and the lower crop suitability threshold. The average fraction of total 2035 jet fuel demand that can be met in each of the four scenarios is 77.6%, 41.1%, 35.9% and 39.6% respectively. Using S1 inputs, 65% of run cases can meet 75% of 2035 US jet fuel demand, and 100% of S1 run cases can meet 50% of demand. However, zero run cases using S2, S3 or S4 inputs can meet 50% of demand. The uncertainty in SAF production potential in run cases from each scenario is due to irrigated and rainfed crop yield uncertainties and feedstock-to-jet conversion efficiency uncertainties. The average amount of SAF produced by each feedstock type in each scenario when production is maximized is shown in Figure 3-1. An average of 6.42, 6.08, 6.05 and 6.10 billion gallons of SAF is derived from residues and wastes in scenarios S1, S2, S3, and S4 respectively.

Additionally, 81.2, 30.7, 21.6, and 27.8 million acres of pastureland is converted to cropland when SAF production is maximized in scenarios S1, S2, S3, and S4 respectively.

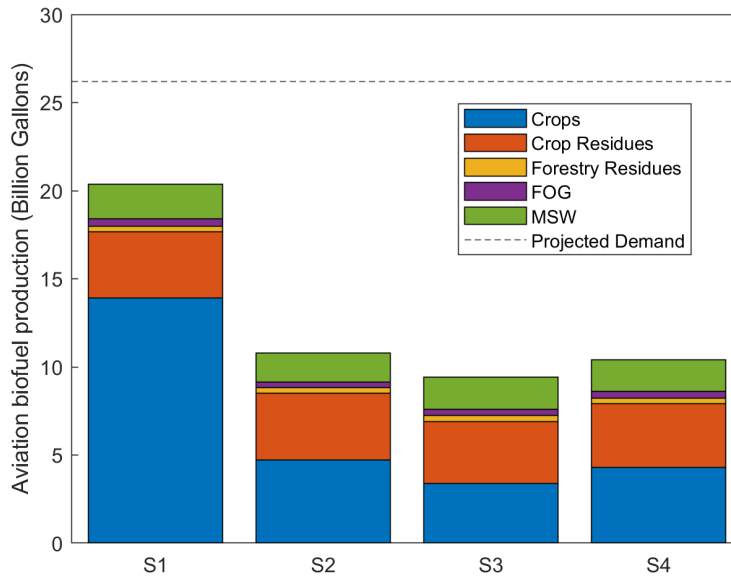


Figure 3-1. Average SAF production potential in each scenario.

3.2 Baseline Optimization Scenario Results

In this section, we present the results from the supply chain optimization using baseline S1 inputs at both carbon costs and both levels of demand.

3.2.1 Carbon Pricing Sensitivity Results

In this section we compare the optimization results with and without a carbon emissions cost from S1 inputs when the demand at each county is 50% of projected 2035 demand. The averages and 95% confidence intervals of the costs and emissions along each step of the optimized supply chain for each of the 100 cases without a carbon cost and the 100 cases with a carbon cost using S1 inputs at 50% demand are shown in Table 3-2. We note that supply chain costs do not include carbon emissions costs.

Table 3-2. Mean and 95% confidence intervals of the costs and emissions along the SAF supply chain using S1 inputs with and without carbon costs.

	0 \$/tonne CO ₂ e		100 \$/tonne CO ₂ e	
	Costs (\$ Billion)	Emissions (Million tonnes CO ₂ e)	Costs (\$ Billion)	Emissions (Million tonnes CO ₂ e)
Land use change	2.4 [2.1-2.8]	30.1 [23.7-36.3]	1.8 [1.4-2.3]	16.4 [7.3-24.3]
Feedstock production	13.3 [11.6-16.0]	24.7 [22.6-28.1]	11.3 [8.7-15.1]	19.6 [15.5-23.4]
Feedstock transportation	1.6 [1.2-2.2]	1.0 [0.8-1.3]	1.7 [1.3-2.4]	1.1 [0.9-1.4]
Refinery costs/emissions	18.7 [15.1-22.2]	27.6 [20.2-34.3]	22.7 [19.6-26.6]	16.7 [7.7-25.1]
Jet transportation	1.25 [1.19-1.30]	0.83 [0.80-0.87]	1.26 [1.21-1.30]	0.82 [0.79-0.84]
Jet combustion		8.0 [7.0-8.9]		8.0 [7.0-8.9]
Total	37.2 [31.8-44.0]	92.2 [78.3-107.4]	38.7 [33.8-44.6]	62.6 [40.7-81.3]

The average per-unit SAF emissions across the entire supply chain for the 100 cases without a carbon cost and the 100 cases with a carbon cost are 54.1 gCO₂e/MJ and 36.6 gCO₂e/MJ respectively, while the average unit SAF cost is 0.75 \$/L and 0.78 \$/L respectively. These values are 39% and 59% lower than the baseline petroleum-derived jet fuel life cycle emissions of 89.0 gCO₂e/MJ, and 50% and 56% higher than the 2019 market jet fuel price of 0.50 \$/L [7,68]. The average unit GHG abatement cost for S1 cases without a carbon cost meeting 50% of demand is 210 \$/tonne CO₂e, while the average abatement cost for cases with a 100 \$/tonne carbon cost is 158 \$/tonne CO₂e.

These unit cost and unit emission values and the results from Table 3-2 indicate that the introduction of a carbon cost in the optimization drives the optimal supply chain towards lower emission feedstocks and pathways that are more capital intensive. When a carbon cost of 100 \$/tonne is introduced, the average total land use change emissions, feedstock production emissions and refinery related emissions decrease by 45.5%, 20.6% and 39.5% respectively, while the average total refinery related costs increase by 21.4%. The average avoided GHG emissions from replacing 50% of 2035 conventional jet fuel demand with SAF is 59.4 million tonnes and 89.2 million tonnes in cases without and with a 100 \$/tonne carbon cost respectively.

Histogram plots showing the distribution of total supply chain costs, total supply chain emissions and unit GHG abatement costs for both of these cases are shown in Figure C-1 in Appendix C . To evaluate the sensitivity of the results to more optimization run cases, we compared the results of 100 runs of the S1 50% demand zero carbon cost case with 100 additional runs of the same scenario and found that the average total supply chain cost, total supply chain emissions and unit GHG abatement cost changed by less than one percent. The distributions of these results for the 200 runs is shown in Figure C-2.

The optimal supply chain configurations for one representative run case using Scenario 1 inputs, meeting 50% of demand and a carbon cost of 0 \$/tonne and 100 \$/tonne are shown in Figure 3-2. These maps show the optimal location of biorefineries, and the counties in which land is converted from pastureland to cropland. The maps also show the pathways each biorefinery uses and the dominant crop grown on the converted land in each county. A map of the optimal supply chain for this run case including airport locations is shown in Figure C-3.

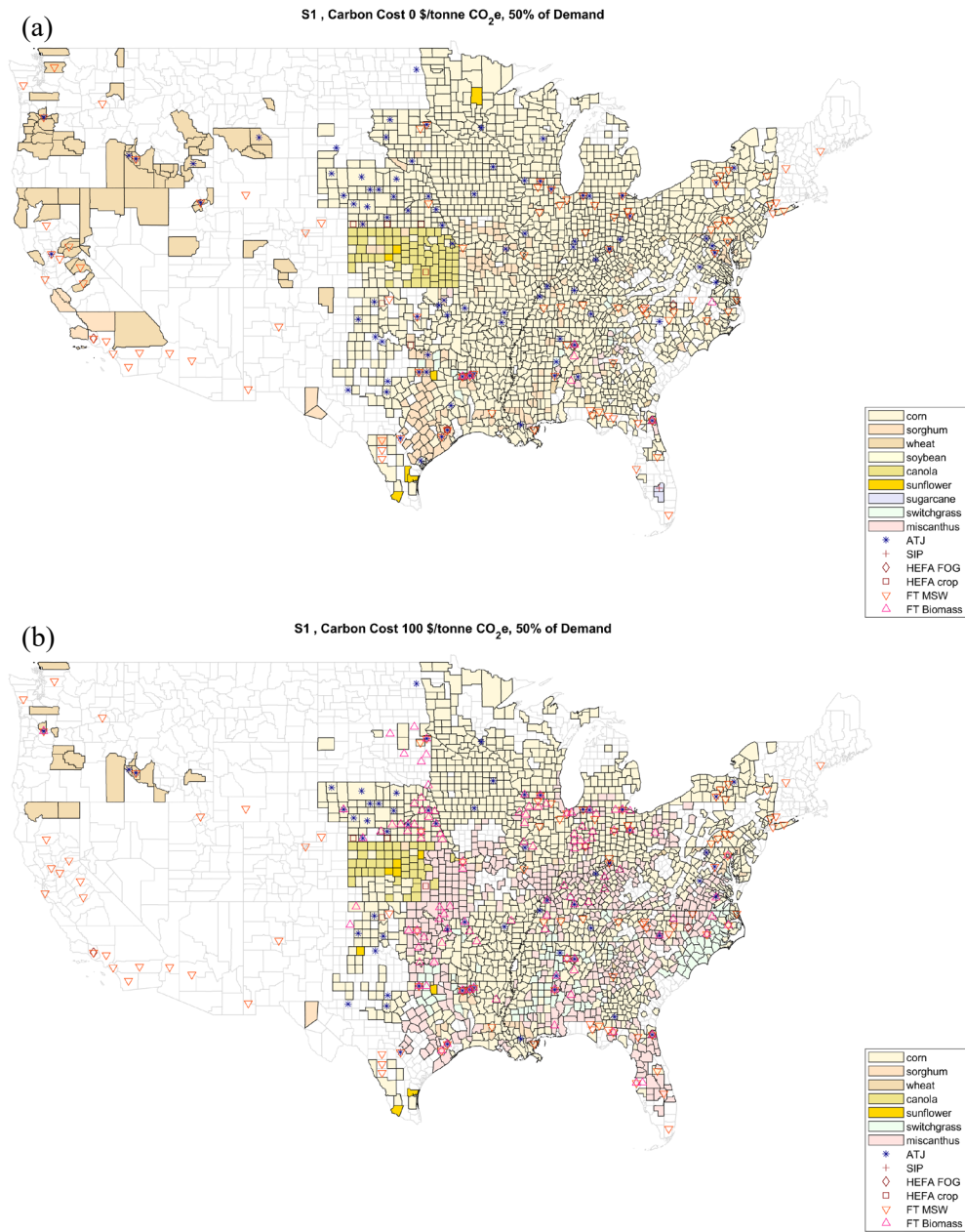


Figure 3-2. Optimal supply chain configurations for one run using S1 inputs meeting 50% of demand without (a) and with (b) a carbon emissions cost.

Although Figure 3-2 is only representative of one set of random S1 inputs, the maps demonstrate that when a carbon cost is introduced into the optimization problem, the minimum cost optimal supply chain uses different feedstocks and pathways to fulfill jet fuel demand. This is further shown in Figure 3-3

which shows the distribution of SAF produced by each feedstock in each of the 100 optimization runs with and without a carbon cost.

The results in Figure 3-3 also demonstrate that there is uncertainty in the optimal SAF supply chain configuration in both scenarios with and without a carbon emissions cost, due to the uncertainty associated with the optimization model inputs such as crop yields and refinery capital costs. Additionally, despite the uncertainty in these key inputs, the results in Figure 3-3 show that the introduction of a carbon cost reduces uncertainty in the quantity of SAF produced via the FT pathway with crop residues. The standard deviation of the volume of SAF produced with crop residue in the 100 cases with a carbon cost is 31% lower than the standard deviation in the cases without a carbon cost.

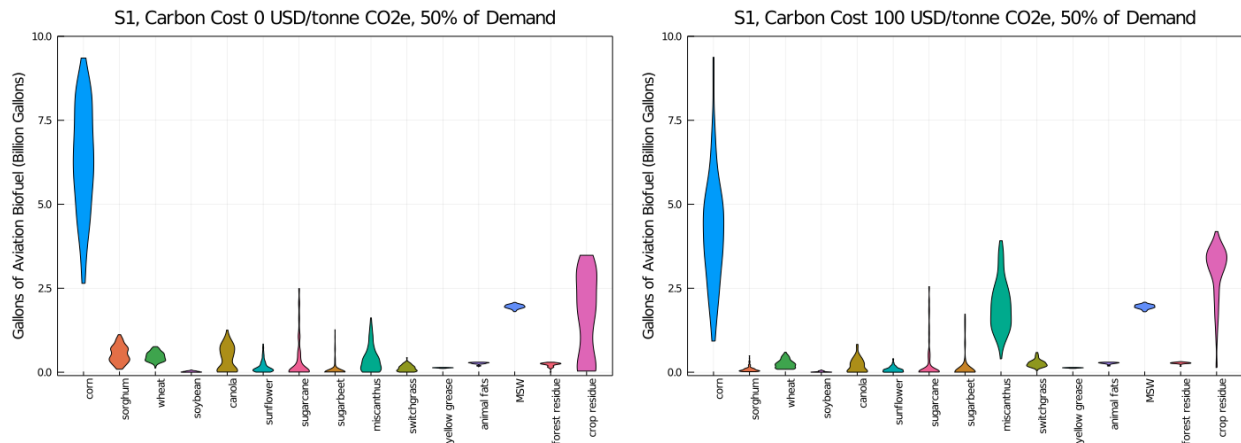


Figure 3-3. Distribution of SAF produced from each feedstock in S1 50% demand optimization cases.

In both cases with and without a carbon cost, the most SAF is produced via the ATJ pathway using corn as the feedstock, with an average of 48.2% and 31.8% of SAF produced via corn ATJ. When a carbon cost is introduced, the optimization drives SAF production towards the FT biomass pathway. This is because the FT biomass pathway has lower life cycle emissions but higher capital costs than the other pathways considered in this analysis. Averages and 95% confidence intervals for average unit costs and unit emissions for SAF produced by each pathway across the entire US supply chain in each of the 100 runs using S1 inputs at 50% demand and no carbon cost are shown in Table C-1.

The average and 95% confidence intervals of SAF production from each pathway in cases with and without a carbon cost is shown in Table 3-3. The results in Table 3-3 and Figure 3-3 show that the amount of MSW and waste greases used for SAF production is maximized regardless of carbon emissions pricing, due to the low costs and low emissions associated with the FT MSW and HEFA FOG pathways. The average refinery size across all pathways and both carbon costs is 9700 BPD, which indicates that the optimization takes advantage of economies of scale to reduce overall costs. The median number of refineries used in the cases with and without a carbon cost is 323 and 271 respectively. The cases with a carbon cost require more refineries because the fraction of jet fuel produced via the FT Biomass pathway is lower than that of the ATJ pathway. More information about the number of refineries built in each scenario is shown in Table C-2. Average state-level SAF production sorted by pathway from 100 optimization runs using S1 inputs at 50% of projected demand with no carbon cost is shown in Table C-3.

Table 3-3. Average and 95% confidence interval of SAF produced from each pathway in S1 50% demand optimization results.

	0 \$/tonne CO₂e	100 \$/tonne CO₂e
Pathway	SAF produced (Billion gallons)	SAF produced (Billion gallons)
ATJ	7.33 [4.32-9.92]	4.52 [1.97-7.31]
HEFA Crop	0.60 [0.00-1.58]	0.30 [0.00-0.73]
SIP	0.40 [0.00-1.78]	0.43 [0.00-2.09]
FT Biomass	2.44 [0.15-5.12]	5.52 [2.95-8.04]
HEFA FOG	0.40 [0.31-0.43]	0.39 [0.31-0.43]
FT MSW	1.95 [1.84-2.04]	1.95 [1.84-2.04]

Additionally, the increase in SAF production from miscanthus, switchgrass, and crop residue drives the 45.5% decrease in LUC emissions in the cases with a carbon cost. There are no LUC emissions associated with crop residue production, and the LUC emissions associated with converting pastureland to cropland for switchgrass or miscanthus are significantly lower than the LUC emissions associated with converting pastureland to cropland for annual crops [43]. Between cases with no carbon cost and cases with a 100

\$/tonne carbon cost, the average total amount of pastureland converted to cropland decreases 13.3% from 51.3 million acres to 44.5 million acres. This represents a 15.0% or a 13.0% increase in cultivated land area in 2035, based on the USGS projections [22].

3.2.2 Supply Chain Scaling Sensitivity Results

The mean and 95% confidence intervals of results from 100 optimization runs using S1 inputs meeting 25% and 50% of demand with and without a carbon cost are summarized in Table 3-4.

Table 3-4. Mean and 95% confidence intervals of optimization results using S1 inputs.

	0 \$/tonne CO₂e		100 \$/tonne CO₂e	
	25% Demand	50% Demand	25% Demand	50% Demand
Costs (\$B)	15.4 [13.4-17.8]	37.2 [31.8-44.0]	16.5 [14.4-19.2]	38.7 [33.8-44.6]
Emissions (Million tonnes CO ₂ e)	43.3 [33.1-49.6]	92.2 [78.3-107.4]	23.6 [13.1-38.2]	62.6 [40.7-81.3]
Avoided Emissions (Million tonnes CO ₂ e)	32.6 [26.3-42.7]	59.4 [44.2-73.3]	52.3 [37.7-62.7]	89.2 [70.4-110.9]
Average Unit Cost (\$/L)	0.62 [0.54-0.72]	0.75 [0.64-0.89]	0.67 [0.58-0.77]	0.78 [0.68-0.90]
Average Unit Emissions (gCO ₂ e/MJ)	50.8 [38.9-58.2]	54.1 [46.0-63.0]	27.7 [15.4-44.8]	36.6 [23.9-47.7]
Average Unit Abatement Cost (\$/tonne CO ₂ e)	95 [29-199]	210 [121-353]	79 [40-137]	157 [94-239]

The average total avoided emissions in the 25% demand cases is over half of the average avoided emissions in the 50% demand cases. This indicates that the feedstocks and pathways used to meet the first 25% of demand have both lower costs and lower life cycle emissions than those used to meet the next 25% of demand. This can also be determined by comparing the average unit abatement costs of the 25% demand cases with the 50% demand cases.

The optimization cases meeting 25% of the jet fuel demand with a 100 \$/tonne carbon cost achieve on average 88% of the total avoided emissions in the cases with no carbon cost meeting 50% of demand. This emphasizes the benefit of introducing a carbon cost into the SAF supply chain. As mentioned previously, the carbon emissions cost drives the optimization towards feedstocks and pathways with lower life cycle emissions. This is shown in Figure 3-4, which shows the average SAF production from each feedstock group in each of the S1 scenarios.

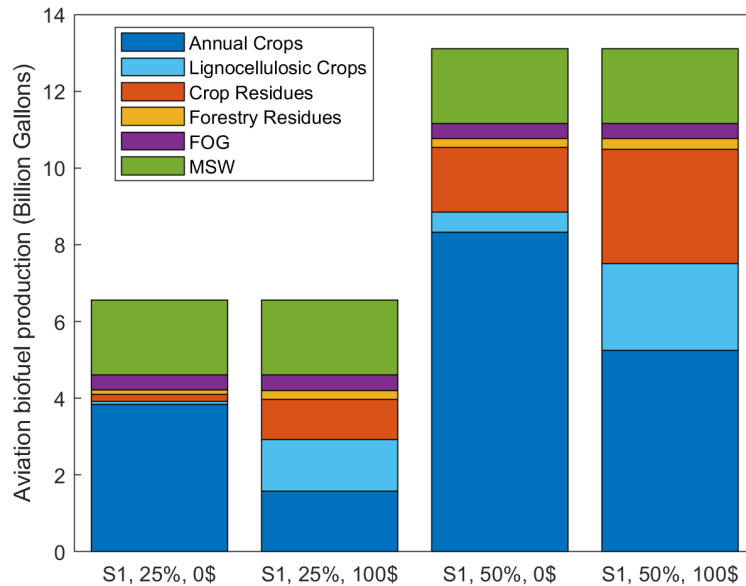


Figure 3-4. Average SAF production from feedstock groups in optimized supply chains using S1 inputs at both demand levels with and without a carbon emissions cost.

The optimal supply chain configurations for one representative run case using Scenario 1 inputs meeting 25% of demand and a carbon cost of 0 \$/tonne and 100 \$/tonne are shown in Figure C-4. The average total pastureland converted to cropland in the cases without a carbon cost increases 158% from 19.9 million acres to 51.3 million acres when demand is increased from 25% to 50% of projected jet demand. In the cases with the carbon cost, the average total pastureland converted to cropland increases 163% from 16.9 million acres to 44.5 million acres.

3.3 Alternative Scenario Results

In this section, we present the results from the supply chain optimization using S2, S3 and S4 inputs meeting 25% of demand with no carbon emissions cost. As shown in Table 3-1, Scenarios 2-4 are unable to meet 50% of 2035 projected jet fuel demand. Therefore, the supply chain optimization was only run with demand set at 25% of projected demand for these scenarios. The mean and 95% confidence intervals of results from 100 optimization runs using S2, S3 and S4 inputs meeting 25% of demand without a carbon cost are summarized in Table 3-5.

Table 3-5. Mean and 95% confidence intervals of optimization results using S2, S3 and S4 inputs meeting 25% of demand with no carbon cost.

Scenario	S2	S3	S4
Costs (\$B)	17.6 [15.3-20.7]	17.6 [15.4-20.6]	17.3 [15.1-20.3]
Emissions (Million tonnes CO ₂ e)	35.2 [22.4-46.6]	29.6 [20.6-39.3]	34.0 [22.0-45.2]
Avoided Emissions (Million tonnes CO ₂ e)	40.7 [29.3-53.4]	46.2 [36.5-55.3]	41.8 [30.7-53.9]
Average Unit Cost (\$/L)	0.71 [0.62-0.83]	0.71 [0.62-0.83]	0.70 [0.61-0.82]
Average Unit Emissions (gCO ₂ e/MJ)	41.3 [26.3-54.6]	34.8 [24.1-46.1]	40.0 [25.8-53.0]
Average Unit Abatement Cost (\$/tonne CO ₂ e)	128 [74-205]	112 [66-177]	118 [67-191]

The land use restrictions in the S2, S3 and S4 scenarios cause the supply chain optimization to convert less pastureland to cropland and use more crop residues and forestry residues, which is similar to the impact of imposing a carbon cost on the supply chain. Compared to the S1 results at the same demand level, the S2, S3 and S4 results have higher costs but lower emissions, resulting in higher average unit abatement costs. The average unit SAF costs from the S1 scenario, which assumes up to 20% of pastureland may be converted to cropland, is 13% lower than the unit SAF costs from the S3 scenario, which is the most restrictive scenario in terms of land availability. However, the unit emissions from the

S3 scenario are 31% lower than the unit emissions from the S1 scenario. The increase in SAF production from residue products is shown in Figure 3-5.

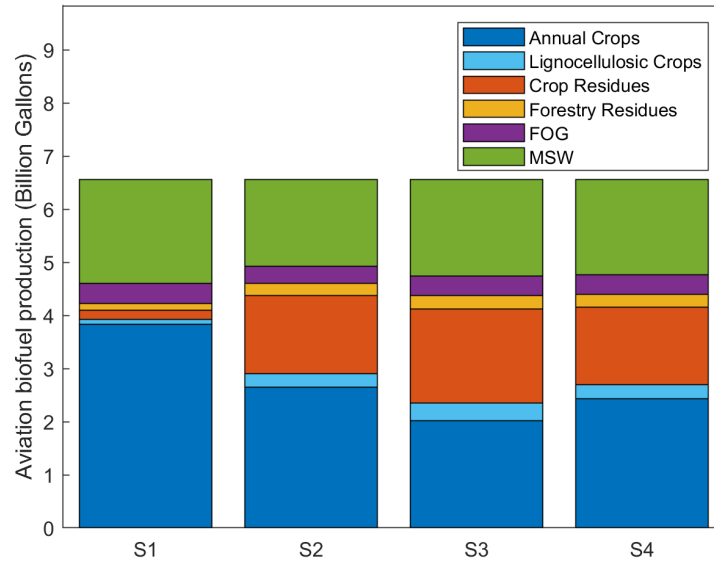


Figure 3-5. Average SAF production from each feedstock group in optimized supply chains using S1, S2, S3 and S4 inputs meeting 25% of demand with no carbon cost.

The average total area of pastureland converted to cropland in the S2, S3 and S4 scenarios are 16.5, 13.8 and 15.6 million acres respectively. Compared to the average of the S1 scenarios meeting 25% of jet fuel demand, this represents up to a 31% reduction in land use change. Additionally, the land use conversion restrictions imposed in the S2, S3 and S4 scenarios causes the geographic extent of land use change to expand compared to the results from the S1 scenario. The average number of counties with a nonzero amount of pastureland converted to cropland in the S1, S2, S3 and S4 scenarios is 1003, 1976, 1910 and 1962 respectively. This is shown in the maps presented in Figure C-5 in Appendix C .

Results from the supply chain optimization using S2, S3 and S4 inputs meeting 25% of demand with a 100 \$/tonne carbon emissions cost are shown in Figure C-6 and Table C-4 in Appendix C . In all cases, the introduction of a carbon emissions cost causes higher supply chain costs, and lower supply chain emissions by producing more SAF via the FT Biomass pathway, which results in lower land use change

emissions, lower feedstock and refinery related emissions, and higher refinery related capital costs. Additionally, in all cases the amount of SAF produced from MSW and FOG is maximized, with differences between scenarios caused by variations in 2035 population projections.

Chapter 4 Conclusions

This study quantifies the potential volume of SAF that can be produced in the US in the year 2035 while evaluating uncertainty in key inputs. The results from this analysis indicate that under a baseline set of assumptions, an average of 78% of 2035 US jet fuel demand can be met with SAF, requiring complete utilization of available waste and residue feedstocks.

This study is the first to optimize the US SAF supply chain using spatially resolved cost and emissions inputs while incorporating regional stochasticity in selected variables. We developed a three-stage supply chain optimization model, and used Monte Carlo simulations to capture uncertainty in the overall supply chain costs and emissions, and optimal feedstock and pathway choices. Under a baseline set of assumptions, when 50% of 2035 US demand is offset, SAF is produced with 50% higher costs and 39% lower emissions than conventional jet fuel. The results also demonstrate that there is uncertainty in the optimal SAF supply chain configuration due to the uncertainty associated with the optimization model inputs such as crop yields and refinery capital costs.

The results from this analysis demonstrate that policies have the ability to impact overall costs and emissions as well as the feedstocks and pathways used in a potential US SAF supply chain. In all scenarios, the introduction of a 100 \$/tonne CO₂e carbon emissions cost caused the optimal supply chains to reduce emissions and increase costs by converting less pastureland to cropland, and by using more crop residues, forestry residues and lignocellulosic crops for SAF production. The introduction of stricter land use restrictions caused similar changes in the optimal supply chains. Additionally, this analysis demonstrates that an increase in a SAF production mandate, from 25% to 50% of 2035 conventional jet fuel demand, results in 21% higher average unit costs, 6% higher unit emissions and 121% higher unit abatement costs.

Future work may consider additional fuel conversion pathways, and may allow feedstocks to be processed using multiple pathways. Further, the framework developed in this analysis can be expanded to evaluate the system wide impacts of additional policies on the SAF supply chain, such as feedstock subsidies and

output based incentives [69]. Finally, future work may expand the life cycle analysis to consider biogeophysical effects, such as the changes in contrail radiative forcing associated with biofuel use, or the climate impacts of surface albedo due to land use change.

Appendix A Pathway Inputs and Outputs

Table A-1. Pathway Inputs and Outputs for ATJ pathway via Ethanol.

			Corn/Sorghum	Wheat	Source
Fermentation to Ethanol	Inputs	Alpha Amylase [g/MJ _{EiOH}]	0.031	0.114	[17,18]
		Gluc Amylase [g/MJ _{EiOH}]	0.067		
		Yeast [g/MJ _{EiOH}]	0.034	0.0002	
		Sulfuric Acid [g/MJ _{EiOH}]	0.058	0.76	
		Ammonia [g/MJ _{EiOH}]	0.22		
		Sodium Hydroxide [g/MJ _{EiOH}]	0.28	0.76	
		Calcium Oxide [g/MJ _{EiOH}]	0.13		
		Natural Gas [MJ/MJ _{EiOH}]	0.319	0.393	
		Electricity [MJ/MJ _{EiOH}]	0.033		
	Outputs	Ethanol [MJ _{EiOH} /dry ton feedstock]	Beta PERT [9380, 9552, 9725]	Uniform [6349, 8720]	[6,17,18,70]
		DDGS [ton/dry US ton feedstock]	0.340	0.345	
		Electricity [MJ/dry ton feedstock]		588	
	Alcohol upgrading to drop-in fuels	Inputs	Ethanol [MJ _{EiOH} /MJ _{Jet}]	Beta PERT [1.075, 1.434, 2.509]	
Electricity [MJ/MJ _{Jet}]			0.033		
Hydrogen [g/MJ _{Jet}]			0.67		
ZSM-5 catalyst [g/MJ _{Jet}]			0.11		
Outputs		Jet [MJ _{Jet}]	1		[17]
		Diesel [MJ _{Diesel} /MJ _{Jet}]	0.12		
		Gasoline [MJ _{Gasoline} /MJ _{Jet}]	0.21		

Table A-2. Pathway Inputs and Outputs for HEFA crop and HEFA FOG pathways.

			Soybean	Canola	Sunflower	FOG	Source	
Oil Extraction	Inputs	Natural Gas [MJ/ dry ton feedstock]	1203.3	1022.1	0		[7,17,19]	
		Electricity [MJ/ dry ton feedstock]	168.7	172.7	172.7			
		Hexane [kg/ dry ton feedstock]	0.477	2.013	2.013			
	Outputs	Crop Oil [ton/dry ton feedstock]	0.215	0.464	0.460			
		Meal [ton/ton oil]	3.5	1.112	1.058			
HEFA processing	Inputs	Oil/FOG [lb./ MJ _{Jet}]	Beta PERT [0.093, 0.098, 0.124]					[5,11]
		Natural Gas [MJ/ lb. oil]	3.39					
		Electricity [MJ/ lb. oil]	0.10					
	Outputs	Jet [MJ _{Jet}]	1					
		Diesel [MJ _{Diesel} /MJ _{Jet}]	0.470					
		Gasoline [MJ _{Gasoline} /MJ _{Jet}]	0.143					
		Lightends [MJ _{Lightends} /MJ _{Jet}]	0.201					

Table A-3. Pathway Inputs and Outputs for SIP Pathway.

		Sugarcane	Sugarbeet	Source
Inputs	Lime [kg/ ton dry feedstock]	2.935		[4,7,72]
	Sulfuric Acid [g/ MJ _{Jet}]		0.155	
	Sodium Carbonate [g/ MJ _{Jet}]		0.045	
	Hydrochloric Acid [g/ MJ _{Jet}]		0.022	
	Formaldehyde [g/ MJ _{Jet}]		0.134	
	Natural Gas [MJ/ MJ _{Jet}]		0.046	
	Hydrogen [g/ MJ _{Jet}]	0.911	0.911	
Outputs	Jet [MJ _{Jet} /dry ton feedstock]	Beta PERT [1974, 3034, 4680]	Beta PERT [3581, 4600, 4958]	
	Electricity [MJ/ dry ton feedstock]	1032	1867	

Table A-4. Pathway Inputs and Outputs for FT Biomass Pathway

		All FT Biomass feedstock	Source
Outputs	Fuel Product [MJ _{Fuel} / MJ _{feedstock}]	Beta PERT [0.42, 0.45, 0.52]	[20]
	Jet [MJ _{Jet} / MJ _{Fuel}]	0.25	
	Diesel [MJ _{Diesel} / MJ _{Fuel}]	0.55	
	Gasoline [MJ _{Gasoline} / MJ _{Fuel}]	0.20	

Table A-5. Pathway Inputs and Outputs for FT MSW Pathway

		MSW	Source
Outputs	Fuel Products [MJ _{Fuel} / MJ _{MSW}]	Beta PERT [0.4970, 0.5354, 0.5716]	[21,73]
	Jet [MJ _{Jet} /MJ _{Fuel}]	0.126	
	Diesel [MJ _{Diesel} /MJ _{Fuel}]	0.762	
	Gasoline [MJ _{Gasoline} /MJ _{Fuel}]	0.112	

Appendix B Additional Model Inputs

Table B-1. 2035 Electricity Emissions Factors for US Census Regions.

Region	Emissions Factor (gCO _{2e} /MJ)
US Average	86.5
New England	25.7
Middle Atlantic	70.1
South Atlantic	73.9
East North Central	128.8
East South Central	96.1
West North Central	129.3
West South Central	97.7
Mountain	103.7
Pacific	23.1

Table B-2. 2035 hydrogen production mixes, costs and emissions factors.

Production Case	Production Method	Emissions Factor (gCO _{2e} /MJ)	Cost (\$/kg H ₂)
Current	100% Natural Gas	94.66	1.26
Reference	87.5% Natural Gas 12.5% Renewables	85.94	1.39
Carbon Constraint	10% Natural Gas 90% Renewables	31.91	2.24

Table B-3. Crop enterprise budgets used in this analysis.

Crop	States	Source
Canola	Kansas, Minnesota, North Dakota, Texas, Wisconsin	[74–78]
Corn	Alabama, Arkansas, California, Colorado, Georgia, Idaho, Indiana, Kansas, Kentucky, Louisiana, Maryland, Minnesota, Mississippi, Missouri, Nebraska, North Carolina, North Dakota, Ohio, South Dakota, Tennessee, Texas	[76–96]
Miscanthus	Illinois, Iowa, Pennsylvania	[97], [98], [99]
Sorghum	Arkansas, California, Colorado, Georgia, Kansas, Kentucky, Louisiana, Maryland, Mississippi, Missouri, Nebraska, North Carolina, Tennessee, Texas	[76,77,79–87,89,90,93]
Soybean	Alabama, Arkansas, Colorado, Georgia, Indiana, Kansas, Kentucky, Louisiana, Maryland, Minnesota, Mississippi, Missouri, Nebraska, North Carolina, North Dakota, Ohio, South Dakota, Tennessee, Texas	[76–91,94–96]
Sugarbeet	Colorado, Idaho, Minnesota, Nebraska, Wyoming	[82,86,92,94,100]
Sugarcane	Louisiana, Texas	[76,90]
Sunflower	California, Colorado, Kansas, Nebraska, North Dakota, South Dakota, Texas	[76–78,82,86,93,95]
Switchgrass	Illinois, Oklahoma, Tennessee	[97,101,102]
Wheat	Arkansas, California, Colorado, Georgia, Idaho, Indiana, Kansas, Kentucky, Louisiana, Maryland, Minnesota, Mississippi, Missouri, Nebraska, North Carolina, North Dakota, Ohio, South Dakota, Tennessee, Texas	[76,77,79–87,90–96]

Table B-4. Feedstock production energy distributions for crops, crop residue and forestry residue

Feedstock	Energy Requirement Distribution (MJ/ dry tonne feedstock)	Energy Inputs	Source
Corn	Weibull (416.4, 6.3)	49% Diesel 18% LPG 15% Gasoline 13% Natural Gas 5% Electricity	[17,103]
Sorghum	Normal (680, 170)	46% Natural Gas 36% Diesel 18% Gasoline	[17,104]
Wheat	Triangular (836, 1020, 1070)	62% Diesel 24% Electricity 14% Gasoline	[17,105]
Soybean	Triangular (701, 821, 1191)	70% Diesel 16% Gasoline 5% Natural Gas 5% Electricity 4% LPG	[17,20]
Canola	Triangular (528, 547, 803)	97% Diesel 3% Electricity	[17,20]
Sunflower	Uniform (1887, 1906)	100% Diesel	[19,106]
Sugarcane	Normal (100, 6.1)	38% Diesel 19% LPG 12% Gasoline 22% Natural Gas 9% Electricity	[17,103]
Sugarbeet	Triangular (141, 208, 380)	59% Diesel 28% Gasoline 13% Electricity	[107]
Miscanthus	Normal (153, 9.1)	93% Diesel 7% Electricity	[17,103]
Switchgrass	Normal (144, 33.4)	100% Diesel	[17,103]
Crop Residue	Normal (219, 13.4)	100% Diesel	[17,103]
Forestry Residue	Normal (267, 35.3)	100% Diesel	[17,108]

Table B-5. Rendering Energy Inputs and Market Prices for FOGs.

Product	Natural Gas Input (MJ/tonne rendered product)	Electricity Input (MJ/tonne rendered product)	Market Prices (\$/tonne)
Yellow Grease	Triangular (290,1460,2240)	Triangular (63,150,250)	Beta PERT (350, 504, 660)
Tallow	Triangular (5490,8390,11500)	Triangular (570,630,1560)	Beta PERT (441, 638, 834)
Poultry Fat	Uniform (7510,8460)	Uniform (709, 738)	Beta PERT (378, 546, 714)
Pork Fat	Uniform (6380,8290)	Uniform (681,703)	Beta PERT (371, 537, 702)

Table B-6. Probability distributions for uncertain cost inputs.

Commodity	Costs
Electricity (\$/kWh)	Triangular (0.0636, 0.0646, 0.0648)
Natural Gas (\$/Mcf)	Triangular (4.29, 4.40, 4.53)
Crude Oil (\$/bbl.)	Triangular (77, 79, 80)

Table B-7. PADD specific fuel price correlations.

Region	Crude (x) to gasoline (\$/bbl. to \$/gal.)	Gasoline (x) to diesel (\$/gal. to \$/gal.)	Gasoline (x) to propane (\$/gal. to \$/gal.)
PADD 1 (East Coast)	$0.0297x + 0.6257$	$1.2011x - 0.2334$	$0.4956x - 0.1078$
PADD 2 (Mid-West)	$0.0292x + 0.6264$	$1.1924x - 0.2364$	$0.4889x - 0.1496$
PADD 3 (Gulf Coast)	$0.0278x + 0.6090$	$1.2386x - 0.2729$	$0.5189x - 0.2106$
PADD 4 (Mountains)	$0.0281x + 0.7284$	$1.2329x - 0.3135$	$0.5216x - 0.2310$
PADD 5 (Pacific)	$0.0311x + 0.8341$	$1.1303x - 0.2462$	$0.5228x - 0.2388$

Table B-8. Deterministic input costs.

Input	Price	Source
Nitrogen fertilizer (\$/lb.)	0.39	[39]
Phosphorus fertilizer (\$/lb.)	0.33	
Potassium fertilizer (\$/lb.)	0.23	
Agricultural lime (Spread) (\$/ton)	38	[109]
Alpha amylase (\$/kg)	3.41	[110]
Gluco amylase (\$/kg)	3.41	
Yeast (\$/kg)	2.81	
Sulfuric acid (\$/kg)	0.13	
Ammonia (\$/kg)	0.65	
Sodium hydroxide (\$/kg)	0.59	
Calcium oxide (\$/kg)	0.29	
ZSM-5 catalyst (\$/kg)	22.71	[111]
Hexane (\$/kg)	0.89	[56]
Sodium carbonate (\$/kg)	0.26	[112]
Hydrochloric acid (\$/kg)	0.12	[113]

Table B-9. Reference capital costs and capacities.

Facility	Deterministic CAPEX (Million USD)	Reference Capacity (Daily BPD)	Source
ATJ	163	2000	[4]
HEFA	68	2000	[10]
Crop Oil Extraction	119	173 (Million kg oil annually)	[56]
SIP	201	2000	[4]
FT Biomass	610	3202	[114]
FT MSW	264	1778	[21]

Table B-10. Costs for each transportation mode.

Transport Mode	Solid Cost (cents/tonne-mile)	Liquid Cost (cents/kgal-mile)
Road	18.83	54.04
Rail	4.23	12.14
Barge	2.94	8.44
Pipeline		Route specific
Transloading Cost	12.35 \$/tonne	40 \$/kgal

Appendix C Additional Results

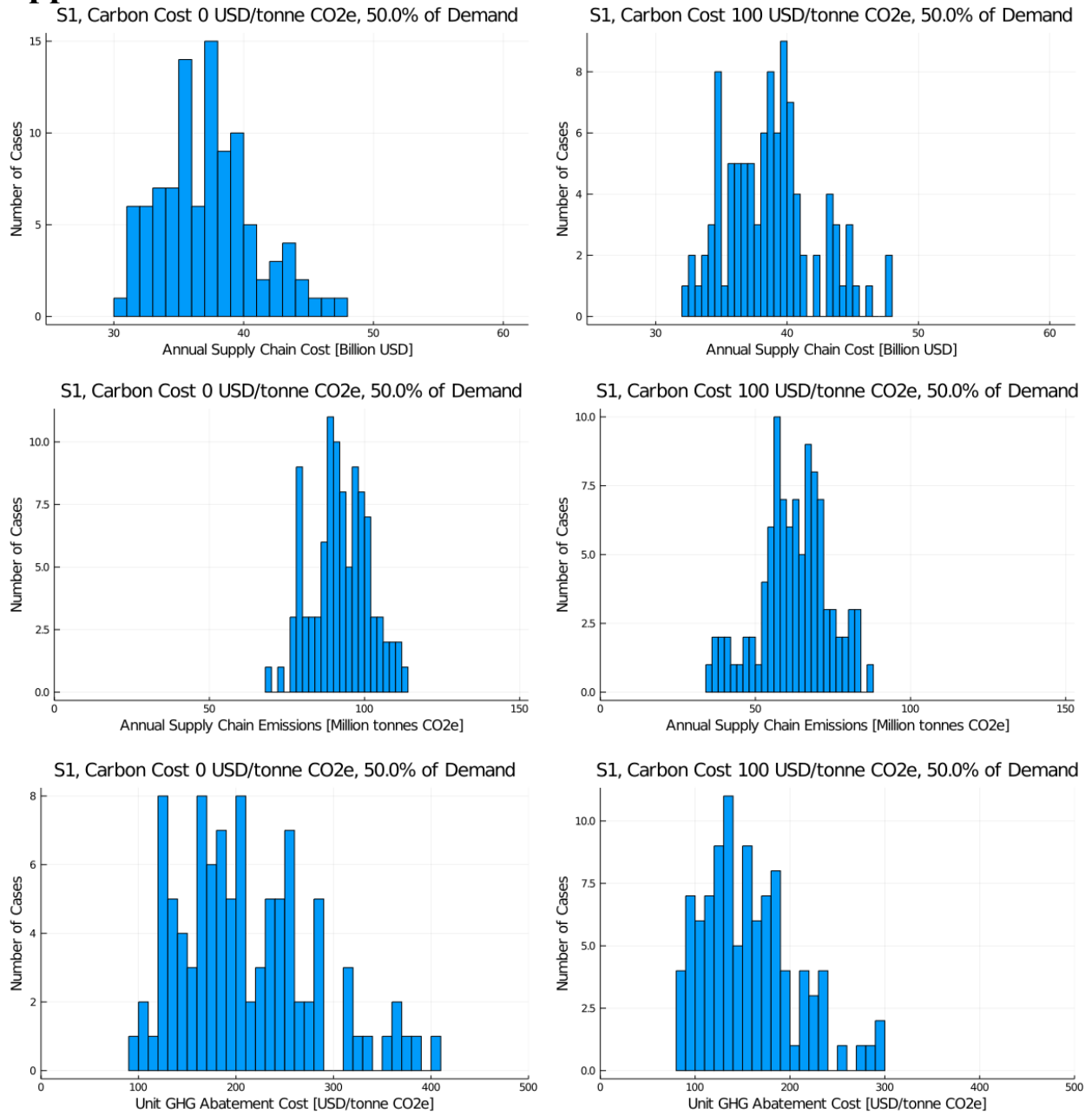


Figure C-1. Distributions of 100 optimization results for total annual costs, total annual emissions, and unit GHG abatement costs for S1 inputs meeting 50% of demand with and without a carbon cost.

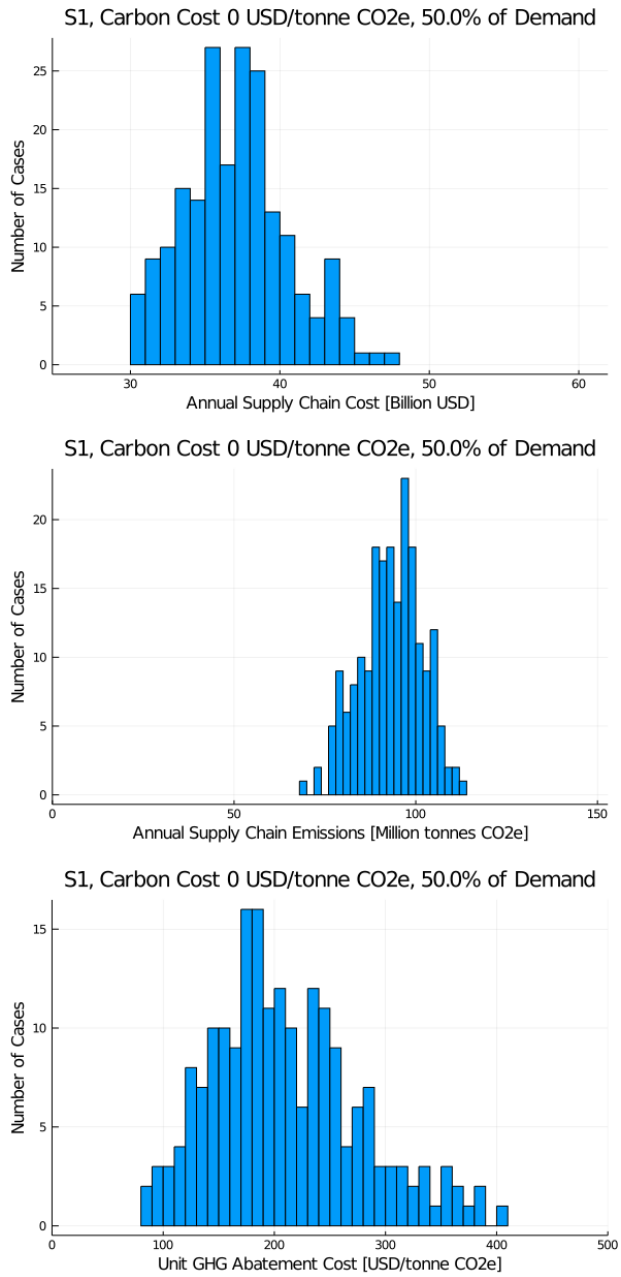


Figure C-2 . Distributions of 200 optimization results for total annual costs, total annual emissions, and unit GHG abatement costs for S1 inputs meeting 50% of demand without a carbon cost.

S1, Carbon Cost 0 \$/tonne CO₂e, 50% of Demand

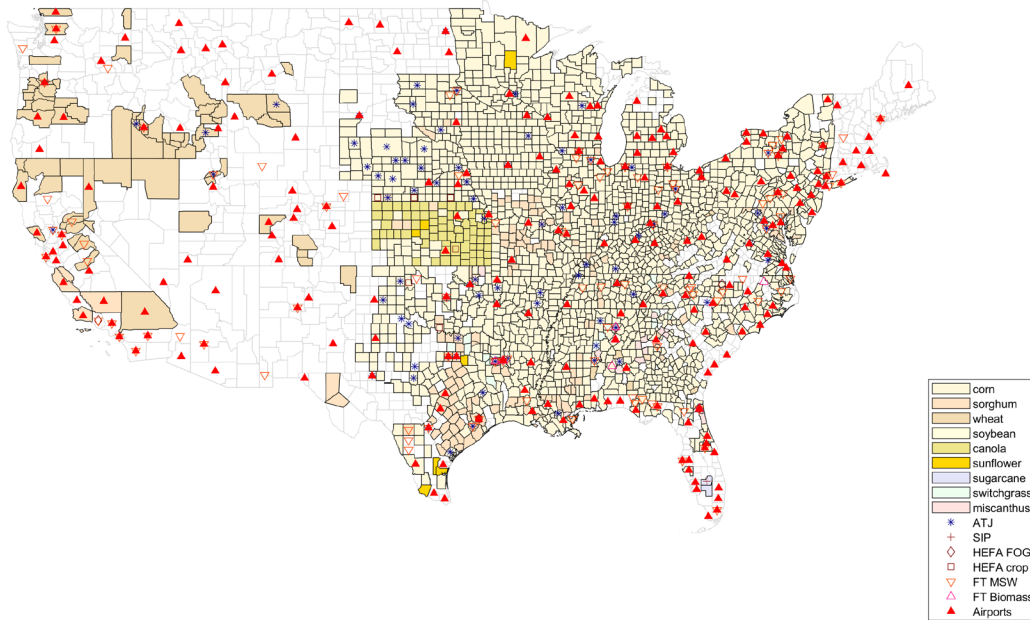


Figure C-3. Optimal supply chain configuration for one run using S1 inputs meeting 50% of demand with airport locations.

Table C-1. Average and 95% confidence intervals for average unit costs and emissions for SAF produced from each pathway in each of the 100 optimized supply chains using S1 inputs at 50% demand and no carbon cost.

Pathway	Unit SAF Cost (\$/L)	Unit SAF Emissions (gCO ₂ e/MJ)
ATJ	0.71 [0.63-0.81]	64.0 [56.5-74.4]
HEFA crop	0.68 [0.59-0.79]	71.7 [60.9-83.5]
HEFA FOG	0.60 [0.49-0.75]	22.7 [21.0-25.0]
SIP	0.84 [0.52-1.14]	49.5 [34.7-67.9]
FT Biomass	0.88 [0.79-1.01]	7.6 [4.4-10.3]
FT MSW	0.36 [0.29-0.46]	25.6 [19.5-31.6]

The unit cost and emissions values include contributions from land use change. The unit cost of SAF via the FT MSW pathway is below the 2019 conventional jet fuel price as a result of large refinery sizes and economies of scale. This was also reported in Niziolek et al 2015 [73].

Table C-2. Summary of median and 95% confidence intervals of refineries built in all scenarios, demand levels, and costs of carbon emissions.

Demand	Scenario	Carbon Cost (\$/tonne CO _{2e})	Number of Refineries						
			Total	ATJ	HEFA crop	HEFA FOG	SIP	MSW	FT Biomass
50%	S1	0	271 [215-320]	72 [44-93]	7 [0-22]	6 [4-6]	1 [0-19]	106 [100-111]	72 [4-144]
		100	323 [275-369]	45 [22-71]	4 [0-11]	6 [4-6]	1 [0-26]	107 [101-111]	157 [81-226]
25%	S1	0	155 [148-184]	32 [19-39]	3 [0-13]	6 [4-6]	0 [0-3]	105 [99-109]	4 [0-50]
		100	204 [160-232]	12 [0-33]	1 [0-7]	6 [5-7]	0 [0-1]	106 [100-110]	75 [16-116]
	S2	0	173 [143-204]	24 [11-40]	2 [0-5]	4 [4-6]	0 [0-4]	88 [83-92]	53 [8-104]
		100	211 [174-235]	8 [0-24]	0 [0-2]	4 [4-6]	0 [0-2]	89 [82-96]	107 [60-129]
	S3	0	187 [163-212]	18 [6-30]	1 [0-4]	5 [4-6]	0 [0-2]	97 [92-103]	65 [26-100]
		100	219 [187-241]	8 [0-19]	0 [0-2]	5 [4-6]	0 [0-2]	100 [94-104]	107 [67-131]
	S4	0	181 [152-209]	22 [10-37]	2 [0-5]	5 [4-6]	0 [0-3]	96 [91-100]	56 [8-94]
		100	217 [181-237]	8 [0-22]	0 [0-2]	5 [4-6]	0 [0-2]	98 [91-102]	108 [61-126]

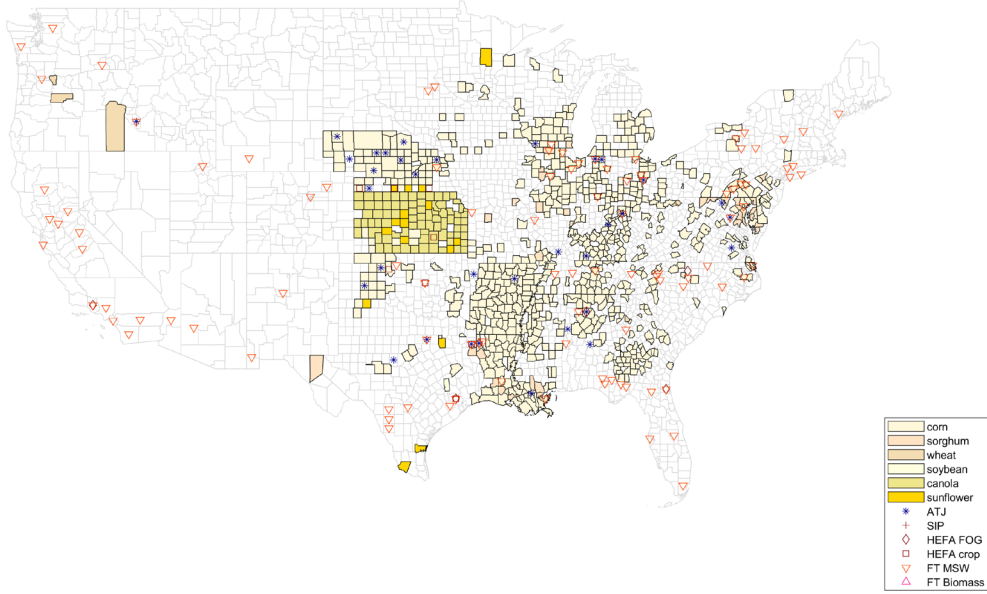
Table C-3. Average SAF production in each US state from 100 optimization runs using S1 inputs at 50% of demand and zero carbon cost.

State	SAF Production (Million Gallons)						
	Total	ATJ	HEFA FOG	HEFA crop	SIP	FT MSW	FT Biomass
Nebraska	2087.92	1469.19	0.00	159.86	0.00	30.98	427.88
Indiana	1937.83	1314.29	74.65	120.10	179.65	150.06	99.07
Illinois	725.38	536.72	0.00	0.00	0.00	18.75	169.91
Texas	664.90	383.23	76.16	0.27	12.75	37.45	155.03
Kentucky	626.01	298.58	0.00	0.00	0.00	74.64	252.79
Alabama	612.93	341.85	0.04	0.00	0.00	89.47	181.57
South Dakota	586.78	343.72	0.00	20.70	0.00	36.04	186.31
Florida	522.14	222.28	0.00	99.04	1.06	37.42	162.33
Oklahoma	473.87	39.75	77.18	0.32	64.68	213.68	78.24
California	472.34	280.76	59.54	0.00	5.89	74.90	51.25
North Carolina	457.98	260.72	0.00	0.00	0.25	91.04	105.97
Ohio	390.22	77.43	36.29	0.32	7.56	167.92	100.71
Louisiana	357.20	55.11	70.84	3.84	0.00	224.81	2.60
New York	348.03	196.81	0.00	0.00	3.80	145.60	1.82
Tennessee	331.24	281.56	0.00	0.24	9.33	18.67	21.44
Arkansas	320.23	241.84	0.00	44.06	0.00	19.18	15.14
Virginia	282.22	222.71	0.42	0.00	4.85	0.00	54.24
West Virginia	220.41	157.15	0.00	41.83	0.00	0.00	21.43
Missouri	202.88	178.00	0.00	0.00	0.00	0.00	24.87
Pennsylvania	175.62	54.52	0.00	0.00	2.57	73.78	44.75
Washington	154.86	105.80	0.00	8.31	0.00	18.73	22.01
North Dakota	151.29	89.67	0.00	61.37	0.00	0.00	0.26
Oregon	117.49	109.33	0.00	0.00	0.00	3.04	5.12
Idaho	109.32	109.32	0.00	0.00	0.00	0.00	0.00
Maryland	96.87	50.19	0.00	16.29	0.00	30.39	0.00
Iowa	91.84	35.17	0.00	0.00	0.00	37.44	19.23
Colorado	84.40	0.00	0.00	0.00	5.99	78.41	0.00
Arizona	83.84	0.00	0.00	23.06	0.00	54.95	5.84
Minnesota	75.57	28.04	0.00	21.56	0.00	18.03	7.94
New Mexico	71.56	34.24	0.00	0.00	0.00	37.32	0.00
Wyoming	59.66	35.71	0.00	0.00	3.56	18.94	1.45
Georgia	39.84	2.73	0.00	0.66	0.00	36.46	0.00
Maine	39.12	0.00	0.00	0.81	0.00	38.00	0.31
Vermont	34.99	0.00	0.00	0.15	0.00	18.74	16.09
Utah	27.34	27.34	0.00	0.00	0.00	0.00	0.00
Connecticut	18.82	0.00	0.00	0.00	0.00	18.76	0.06
Montana	18.76	0.00	0.00	0.00	0.00	18.76	0.00
Kansas	18.54	0.00	0.00	0.00	0.00	18.54	0.00
South Carolina	16.11	0.00	0.00	13.76	0.00	0.00	2.35
Mississippi	6.26	0.00	0.00	0.00	5.90	0.00	0.36
Wisconsin	0.85	0.41	0.00	0.00	0.16	0.00	0.28

Michigan	0.51	0.00	0.00	0.00	0.00	0.00	0.51
Delaware	0.00	0.00	0.00	0.00	0.00	0.00	0.00
Massachusetts	0.00	0.00	0.00	0.00	0.00	0.00	0.00
Nevada	0.00	0.00	0.00	0.00	0.00	0.00	0.00
New Hampshire	0.00	0.00	0.00	0.00	0.00	0.00	0.00
New Jersey	0.00	0.00	0.00	0.00	0.00	0.00	0.00
Rhode Island	0.00	0.00	0.00	0.00	0.00	0.00	0.00

This shows the average geographic distributions of the biorefineries. States without any biofuel production still supply feedstock to refineries in other states.

S1 , Carbon Cost 0 \$/tonne CO₂e, 25% of Demand



S1 , Carbon Cost 100 \$/tonne CO₂e, 25% of Demand

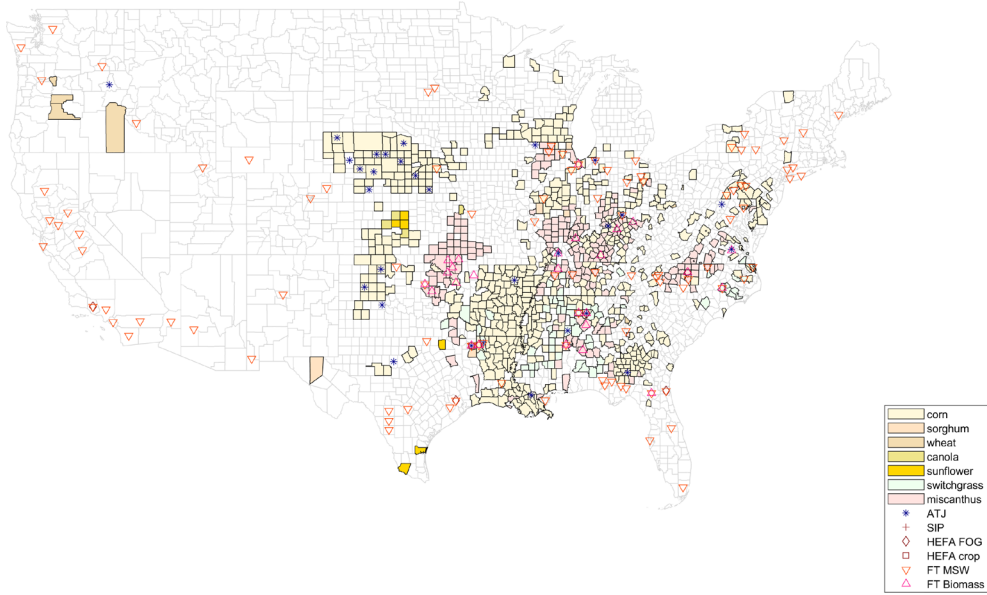


Figure C-4. Optimal supply chain configurations for one run using S1 inputs meeting 25% of demand with and without a carbon emissions cost.

Table C-4. Summary of mean and 95% confidence intervals of optimization results from all scenarios, carbon costs and levels of demand.

Scenario	S1				S2		S3		S4	
	50%		25%		25%		25%		25%	
Carbon Cost (\$/tonne CO ₂ e)	0	100	0	100	0	100	0	100	0	100
Costs (\$B)	37.2 [31.8-44.0]	38.7 [33.8-44.6]	15.4 [13.4-17.8]	16.5 [14.4-19.2]	17.6 [15.3-20.7]	18.3 [16.1-21.3]	17.6 [15.4-20.6]	18.2 [16.0-21.2]	17.3 [15.1-20.3]	18.0 [15.9-21.1]
Emissions (Million tonnes CO ₂ e)	92.2 [78.3-107.4]	62.6 [40.7-81.3]	43.3 [33.1-49.6]	23.6 [13.1-38.2]	35.2 [22.4-46.6]	19.2 [12.7-30.9]	29.6 [20.6-39.3]	18.5 [13.4-26.8]	34.0 [22.0-45.2]	19.0 [12.9-29.6]
Avoided Emissions (Million tonnes CO ₂ e)	59.4 [44.2-73.3]	89.2 [70.4-110.9]	32.6 [26.3-42.7]	52.3 [37.7-62.7]	40.7 [29.3-53.4]	56.6 [44.9-63.1]	46.2 [36.5-55.3]	57.3 [49.1-62.5]	41.8 [30.7-53.9]	56.9 [46.3-62.9]
Average Unit Cost (\$/L)	0.75 [0.64-0.89]	0.78 [0.68-0.90]	0.62 [0.54-0.72]	0.67 [0.58-0.77]	0.71 [0.62-0.83]	0.74 [0.65-0.86]	0.71 [0.62-0.83]	0.73 [0.65-0.85]	0.70 [0.61-0.82]	0.73 [0.64-0.85]
Average Unit Emissions (gCO ₂ e/MJ)	54.1 [46.0-63.0]	36.6 [23.9-47.7]	50.8 [38.9-58.2]	27.7 [15.4-44.8]	41.3 [26.3-54.6]	22.6 [15.0-36.3]	34.8 [24.1-46.1]	21.7 [15.7-31.4]	40.0 [25.8-53.0]	22.3 [15.2-34.7]
Average Unit Abatement Cost (\$/tonne CO ₂ e)	210 [121-353]	157 [94-239]	95 [29-199]	79 [40-137]	128 [74-205]	105 [66-157]	112 [66-177]	101 [63-152]	118 [67-191]	99 [61-152]

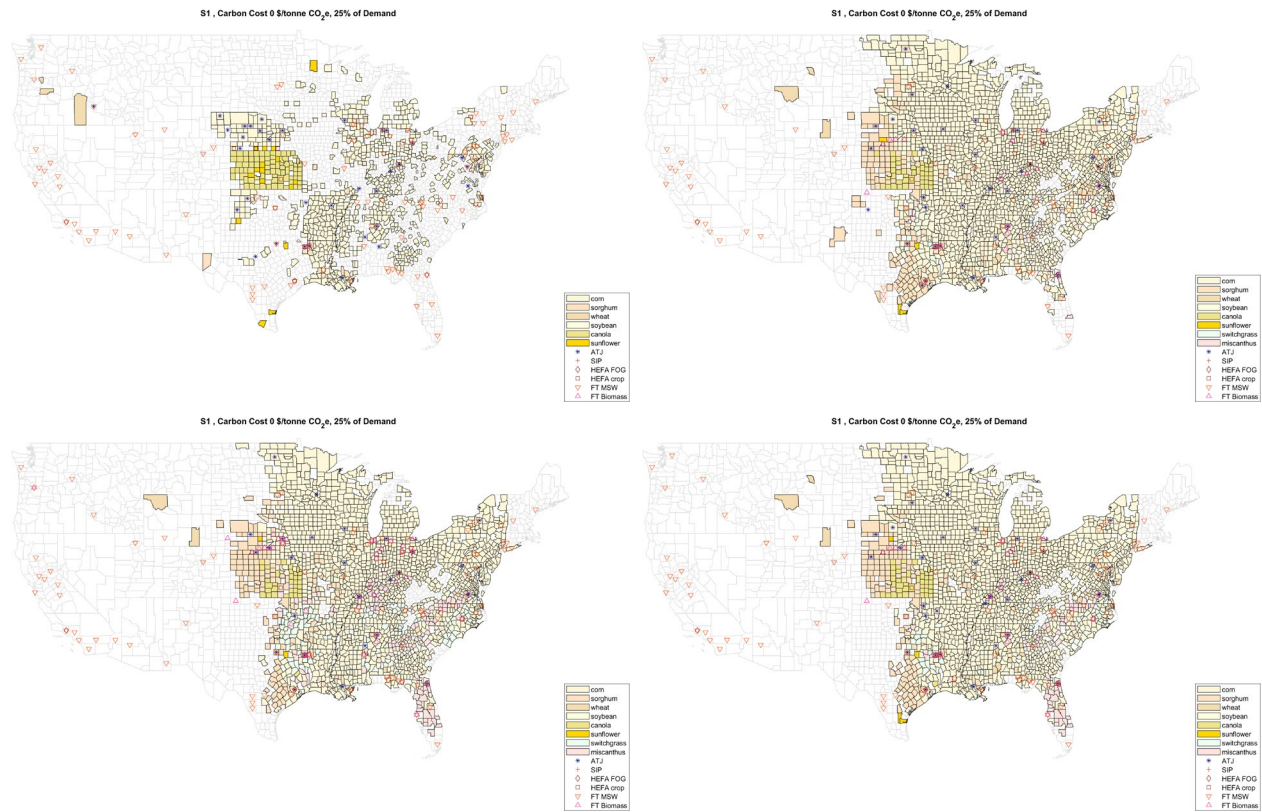


Figure C-5. Optimal supply chain configurations for one run using S1, S2, S3 and S4 inputs meeting 25% of demand with no carbon emissions cost.

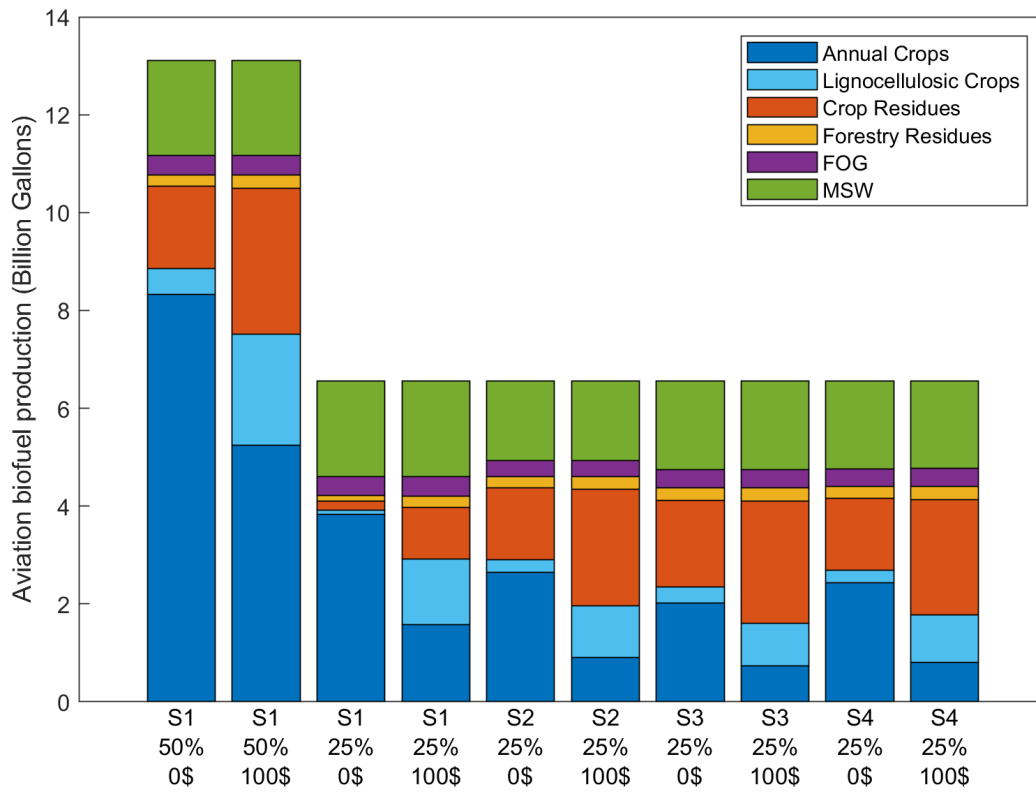


Figure C-6. Average SAF production from each feedstock group from 100 optimization runs using inputs from each scenario, demand level, and carbon emissions cost.

References

- [1] *Inventory of U.S. Greenhouse Gas Emissions and Sinks: 1990-2019*. Publication EPA 430-R-21-005. EPA, 2021.
- [2] Boeing: Commercial Market Outlook. <https://www.boeing.com/commercial/market/commercial-market-outlook/>. Accessed May 23, 2021.
- [3] Doliente, S. S., Narayan, A., Tapia, J. F. D., Samsatli, N. J., Zhao, Y., and Samsatli, S. “Bio-Aviation Fuel: A Comprehensive Review and Analysis of the Supply Chain Components.” *Frontiers in Energy Research*, Vol. 8, 2020. <https://doi.org/10.3389/fenrg.2020.00110>.
- [4] Staples, M. D., Malina, R., Olcay, H., Pearlson, M. N., Hileman, J. I., Boies, A., and Barrett, S. R. H. “Lifecycle Greenhouse Gas Footprint and Minimum Selling Price of Renewable Diesel and Jet Fuel from Fermentation and Advanced Fermentation Production Technologies.” *Energy & Environmental Science*, Vol. 7, No. 5, 2014, pp. 1545–1554. <https://doi.org/10.1039/C3EE43655A>.
- [5] Seber, G., Malina, R., Pearlson, M. N., Olcay, H., Hileman, J. I., and Barrett, S. R. H. “Environmental and Economic Assessment of Producing Hydroprocessed Jet and Diesel Fuel from Waste Oils and Tallow.” *Biomass and Bioenergy*, Vol. 67, 2014, pp. 108–118. <https://doi.org/10.1016/j.biombioe.2014.04.024>.
- [6] Han, J., Tao, L., and Wang, M. “Well-to-Wake Analysis of Ethanol-to-Jet and Sugar-to-Jet Pathways.” *Biotechnology for Biofuels*, Vol. 10, No. 1, 2017, p. 21. <https://doi.org/10.1186/s13068-017-0698-z>.
- [7] CORSIA Supporting Document: CORSIA Eligible Fuels LCA Methodology. https://www.icao.int/environmental-protection/CORSIA/Documents/CORSIA%20Supporting%20Document_CORSIA%20Eligible%20Fuels_LCA%20Methodology.pdf. Accessed May 23, 2021.
- [8] Staples, M. D., Malina, R., Suresh, P., Hileman, J. I., and Barrett, S. R. H. “Aviation CO₂ Emissions Reductions from the Use of Alternative Jet Fuels.” *Energy Policy*, Vol. 114, 2018. <https://doi.org/10.1016/j.enpol.2017.12.007>.
- [9] Galligan, T. *CO₂ Emissions Reduction Potential of Aviation Biofuels in the US*. MS Thesis. Massachusetts Institute of Technology, 2018.
- [10] Bann, S. J., Malina, R., Staples, M. D., Suresh, P., Pearlson, M., Tyner, W. E., Hileman, J. I., and Barrett, S. “The Costs of Production of Alternative Jet Fuel: A Harmonized Stochastic Assessment.” *Bioresource Technology*, Vol. 227, 2017, pp. 179–187. <https://doi.org/10.1016/j.biortech.2016.12.032>.
- [11] Pearlson, M., Wollersheim, C., and Hileman, J. “A Techno-Economic Review of Hydroprocessed Renewable Esters and Fatty Acids for Jet Fuel Production.” *Biofuels, Bioproducts and Biorefining*, Vol. 7, No. 1, 2013, pp. 89–96. <https://doi.org/10.1002/bbb.1378>.
- [12] Lewis, K. C., Newes, E. K., Peterson, S. O., Pearlson, M. N., Lawless, E. A., Brandt, K., Camenzind, D., Wolcott, M. P., English, B. C., Latta, G. S., Malwitz, A., Hileman, J. I., Brown, N. L., and Haq, Z. “US Alternative Jet Fuel Deployment Scenario Analyses Identifying Key Drivers and Geospatial Patterns for the First Billion Gallons.” *Biofuels, Bioproducts and Biorefining*, Vol. 13, No. 3, 2019, pp. 471–485. <https://doi.org/10.1002/bbb.1951>.
- [13] Huang, E., Zhang, X., Rodriguez, L., Khanna, M., de Jong, S., Ting, K. C., Ying, Y., and Lin, T. “Multi-Objective Optimization for Sustainable Renewable Jet Fuel Production: A Case Study of Corn Stover Based Supply Chain System in Midwestern U.S.” *Renewable and Sustainable Energy Reviews*, Vol. 115, 2019, p. 109403. <https://doi.org/10.1016/j.rser.2019.109403>.
- [14] Parker, N., Tittmann, P., Hart, Q., Nelson, R., Skog, K., Schmidt, A., Gray, E., and Jenkins, B. “Development of a Biorefinery Optimized Biofuel Supply Curve for the Western United States.” *Biomass and Bioenergy*, Vol. 34, No. 11, 2010, pp. 1597–1607. <https://doi.org/10.1016/j.biombioe.2010.06.007>.

- [15] *Sustainable Aviation Fuel: Review of Technical Pathways Report*. Publication DOE/EE-2041. DOE, 2020.
- [16] Wang, M., Huo, H., and Arora, S. “Methods of Dealing with Co-Products of Biofuels in Life-Cycle Analysis and Consequent Results within the U.S. Context.” *Energy Policy*, Vol. 39, No. 10, 2011, pp. 5726–5736. <https://doi.org/10.1016/j.enpol.2010.03.052>.
- [17] *Greenhouse Gases, Regulated Emissions, and Energy Use in Technologies (GREET) Model*. Argonne National Laboratory, 2020.
- [18] Lantz, M., Prade, T., Ahlgren, S., and Björnsson, L. “Biogas and Ethanol from Wheat Grain or Straw: Is There a Trade-Off between Climate Impact, Avoidance of ILUC and Production Cost?” *Energies*, Vol. 11, No. 10, 2018, p. 2633. <https://doi.org/10.3390/en11102633>.
- [19] Schmidt, J. H. “Life Cycle Assessment of Five Vegetable Oils.” *Journal of Cleaner Production*, Vol. 87, 2015, pp. 130–138. <https://doi.org/10.1016/j.jclepro.2014.10.011>.
- [20] Stratton, R., Hsin Min Wong, and James Hileman. *Life Cycle Greenhouse Gas Emissions from Alternative Jet Fuels*. Publication PARTNER-COE-2010-001. 2010.
- [21] Suresh, P., Malina, R., Staples, M. D., Lizin, S., Olcay, H., Blazy, D., Pearlson, M. N., and Barrett, S. R. H. “Life Cycle Greenhouse Gas Emissions and Costs of Production of Diesel and Jet Fuel from Municipal Solid Waste.” *Environmental Science & Technology*, Vol. 52, No. 21, 2018, pp. 12055–12065. <https://doi.org/10.1021/acs.est.7b04277>.
- [22] Sohl, T. L., Saylor, K. L., Bouchard, M. A., Reker, R. R., Friesz, A. M., Bennett, S. L., Sleeter, B. M., Sleeter, R. R., Wilson, T., Soulard, C., Knappe, M., and Hofwegen, T. V. “Spatially Explicit Modeling of 1992–2100 Land Cover and Forest Stand Age for the Conterminous United States.” *Ecological Applications*, Vol. 24, No. 5, 2014, pp. 1015–1036. <https://doi.org/10.1890/13-1245.1>.
- [23] *Global Agro-Ecological Zones (GAEZ v3.0)*. IIASA/FAO, IIASA, Laxenburg, Austria and FAO, Rome, Italy, 2012.
- [24] USDA/NASS QuickStats Ad-Hoc Query Tool. <https://quickstats.nass.usda.gov/>. Accessed May 23, 2021.
- [25] M. H. Langholtz, B. J. Stokes, and L. M. Eaton. *2016 Billion-Ton Report: Advancing Domestic Resources for a Thriving Bioeconomy, Volume 1: Economic Availability of Feedstocks*. Publication ORNL/TM-2016/160. Oak Ridge National Laboratory, 2016.
- [26] Lal, R. “World Crop Residues Production and Implications of Its Use as a Biofuel.” *Environment International*, Vol. 31, No. 4, 2005, pp. 575–584. <https://doi.org/10.1016/j.envint.2004.09.005>.
- [27] CropScape - NASS CDL Program. <https://nassgeodata.gmu.edu/CropScape/>. Accessed May 23, 2021.
- [28] Muth, D. J., Bryden, K. M., and Nelson, R. G. “Sustainable Agricultural Residue Removal for Bioenergy: A Spatially Comprehensive US National Assessment.” *Applied Energy*, Vol. 102, 2013, pp. 403–417. <https://doi.org/10.1016/j.apenergy.2012.07.028>.
- [29] Hauer, M. E. “Population Projections for U.S. Counties by Age, Sex, and Race Controlled to Shared Socioeconomic Pathway.” *Scientific Data*, Vol. 6, No. 1, 2019, p. 190005. <https://doi.org/10.1038/sdata.2019.5>.
- [30] Milbrandt, A., Seiple, T., Heimiller, D., Skaggs, R., and Coleman, A. “Wet Waste-to-Energy Resources in the United States.” *Resources, Conservation and Recycling*, Vol. 137, 2018, pp. 32–47. <https://doi.org/10.1016/j.resconrec.2018.05.023>.
- [31] Moore, T., and Myers, E. H. *An Assessment of the Restaurant Grease Collection and Rendering Industry in South Carolina*. Publication SERBEP-SSEB2003MO-MSA-001. US Department of Energy, 2010.
- [32] *USDA Agricultural Projections to 2029*. Publication Long-term Projections Report OCE-2020-1. USDA, 2020.
- [33] USDA. “Poultry Slaughter 2017 Summary.” 2018.
- [34] Hoornweg, D., and Bhada-Tata, P. *What a Waste: A Global Review of Solid Waste Management*. World Bank, Washington, DC, 2012.

- [35] *Advancing Sustainable Materials Management: 2014 Fact Sheet*. Publication EPA530-R-17-01. EPA, 2016.
- [36] Annual Energy Outlook 2020. <https://www.eia.gov/outlooks/aeo/>. Accessed May 23, 2021.
- [37] Margaret Singh, Jim Moore, and William Shadis. Hydrogen Demand, Production, and Cost by Region to 2050. <https://publications.anl.gov/anlpubs/2005/09/54462.pdf>. Accessed May 23, 2021.
- [38] “World Energy Outlook 2006.” 2006, p. 601.
- [39] USDA ERS - Documentation and Data Sources. <https://www.ers.usda.gov/data-products/fertilizer-use-and-price/documentation-and-data-sources/>. Accessed May 23, 2021.
- [40] Chatterjee, A. “Annual Crop Residue Production and Nutrient Replacement Costs for Bioenergy Feedstock Production in United States.” *Agronomy Journal*, Vol. 105, No. 3, 2013, pp. 685–692. <https://doi.org/10.2134/agronj2012.0350>.
- [41] López, D. E., Mullins, J. C., and Bruce, D. A. “Energy Life Cycle Assessment for the Production of Biodiesel from Rendered Lipids in the United States.” *Industrial & Engineering Chemistry Research*, Vol. 49, No. 5, 2010, pp. 2419–2432. <https://doi.org/10.1021/ie900884x>.
- [42] *Emission Factor Documentation for AP-42: Section 9.5.3: Meat Rendering Plants*. Publication MRI Project No. 4602-03. EPA, 1995.
- [43] Taheripour, F., Zhao, X., and Tyner, W. E. “The Impact of Considering Land Intensification and Updated Data on Biofuels Land Use Change and Emissions Estimates.” *Biotechnology for Biofuels*, Vol. 10, No. 1, 2017, p. 191. <https://doi.org/10.1186/s13068-017-0877-y>.
- [44] State Electricity Profiles - Energy Information Administration. <https://www.eia.gov/electricity/state/>. Accessed May 23, 2021.
- [45] Natural Gas Industrial Price. https://www.eia.gov/dnav/ng/ng_pri_sum_a_epg0_pin_dmcf_a.htm. Accessed May 23, 2021.
- [46] PADD Regions Enable Regional Analysis of Petroleum Product Supply and Movements - U.S. Energy Information Administration (EIA). <https://www.eia.gov/todayinenergy/detail.php?id=4890>. Accessed May 23, 2021.
- [47] Parkinson, B., Balcombe, P., F. Speirs, J., D. Hawkes, A., and Hellgardt, K. “Levelized Cost of CO₂ Mitigation from Hydrogen Production Routes.” *Energy & Environmental Science*, Vol. 12, No. 1, 2019, pp. 19–40. <https://doi.org/10.1039/C8EE02079E>.
- [48] IRENA. “Hydrogen: A Renewable Energy Perspective.” 2019.
- [49] Commodity Costs and Returns - USDA ERS. <https://www.ers.usda.gov/data-products/commodity-costs-and-returns/commodity-costs-and-returns/#Historical%20Costs%20and%20Returns:%20Corn>. Accessed May 23, 2021.
- [50] Gallagher, P., Dikeman, M., Fritz, J., Wailes, E., Gauthier, W., and Shapouri, H. *Biomass from Crop Residues: Cost and Supply Estimates*. Publication Agricultural Economic Report No. 819. USDA, Washington, DC, 2003.
- [51] Plastina, A. “2021 Iowa Farm Custom Rate Survey.” 2021, p. 5.
- [52] U.S. Bureau of Labor Statistics. Producer Price Index by Commodity: Chemicals and Allied Products: Lard, Inedible Tallow, and Grease, Except Wool Grease. *FRED, Federal Reserve Bank of St. Louis*. <https://fred.stlouisfed.org/series/WPU06410132>. Accessed May 23, 2021.
- [53] Swisher, K. Market Report: Ups and Downs All Around. *Render Magazine*, Apr, 2017, pp. 10–15.
- [54] The Chemical Engineering Plant Cost Index - Chemical Engineering. <https://www.chemengonline.com/pci-home>. Accessed May 23, 2021.
- [55] Tsagakari, M., Couturier, J.-L., Kokossis, A., and Dubois, J.-L. “Early-Stage Capital Cost Estimation of Biorefinery Processes: A Comparative Study of Heuristic Techniques.” *ChemSusChem*, Vol. 9, No. 17, 2016, pp. 2284–2297. <https://doi.org/10.1002/cssc.201600309>.
- [56] Cheng, M.-H., and Rosentrater, K. A. “Economic Feasibility Analysis of Soybean Oil Production by Hexane Extraction.” *Industrial Crops and Products*, Vol. 108, 2017, pp. 775–785. <https://doi.org/10.1016/j.indcrop.2017.07.036>.

- [57] WACC. *gurufocus*. <https://www.gurufocus.com/term/wacc/NYSE:WPX/WACC-/WPX-Energy>. Accessed May 23, 2021.
- [58] Watson, G. Combined State and Federal Corporate Income Tax Rates in 2020. Tax Foundation, , 2020.
- [59] Area Cost Factors. *US Army Corps of Engineers*. <https://www.usace.army.mil/Cost-Engineering/Area-Cost-Factors/>. Accessed May 23, 2021.
- [60] Average Freight Revenue per Ton-Mile. *United States Department of Transportation Bureau of Transportation Statistics*. <https://www.bts.gov/content/average-freight-revenue-ton-mile>. Accessed May 23, 2021.
- [61] Lewis, K., Matthew N. Pearlson, Alexander Oberg, Olivia Gillham, Scott Smith, Gary Baker, Michelle Gilmore, Amro El-Adle, and Mark Mockett. *Freight and Fuel Transportation Optimization Tool Technical Documentation: FTOT 2020.4 Public Release Version*. John A Volpe National Transportation Systems Center, Cambridge, MA, 2020.
- [62] Dietrich, J. P., Bodirsky, B. L., Weindl, I., Humpenöder, F., Stevanovic, M., Kreidenweis, U., Wang, X., Karstens, K., Mishra, A., Beier, F. D., Molina Bacca, E. J., von Jeetze, P., Windisch, M., Crawford, M. S., Klein, D., Ambrósio, G., Araujo, E., Biewald, A., Lotze-Campen, H., and Popp, A. “MAGPIE - An Open Source Land-Use Modeling Framework.” 2021. <https://doi.org/10.5281/zenodo.4730378>.
- [63] Kreidenweis, U., Humpenöder, F., Kehoe, L., Kuemmerle, T., Bodirsky, B. L., Lotze-Campen, H., and Popp, A. “Pasture Intensification Is Insufficient to Relieve Pressure on Conservation Priority Areas in Open Agricultural Markets.” *Global Change Biology*, Vol. 24, No. 7, 2018, pp. 3199–3213. <https://doi.org/10.1111/gcb.14272>.
- [64] Worldwide, O. A. Flight Schedule Database | Airline Database | OAG. <https://www.oag.com/airline-schedules-data>. Accessed May 23, 2021.
- [65] Simone, N. W., Stettler, M. E. J., and Barrett, S. R. H. “Rapid Estimation of Global Civil Aviation Emissions with Uncertainty Quantification.” *Transportation Research Part D: Transport and Environment*, Vol. 25, 2013, pp. 33–41. <https://doi.org/10.1016/j.trd.2013.07.001>.
- [66] Zheng, S., and Rutherford, D. *Fuel Burn of New Commercial Jet Aircraft: 1960 to 2019*. The International Council on Clean Transportation, 2020, p. 25.
- [67] Denicoff, M., Prater, M. E., and Bahizi, P. *Corn Transportation Profile*. U.S. Department of Agriculture, Agricultural Marketing Service, 2014.
- [68] Spot Prices for Crude Oil and Petroleum Products. *EIA*. https://www.eia.gov/dnav/pet/pet_pri_spt_s1_d.htm. Accessed May 25, 2021.
- [69] Z. Juju Wang. *Quantitative Policy Analysis for Aviation Biofuel Production Technologies*. MS Thesis. Massachusetts Institute of Technology, 2019.
- [70] Buchspies, B., and Kaltschmitt, M. “Life Cycle Assessment of Bioethanol from Wheat and Sugar Beet Discussing Environmental Impacts of Multiple Concepts of Co-Product Processing in the Context of the European Renewable Energy Directive.” *Biofuels*, Vol. 7, No. 2, 2016, pp. 141–153. <https://doi.org/10.1080/17597269.2015.1122472>.
- [71] Yao, G., Staples, M. D., Malina, R., and Tyner, W. E. “Stochastic Techno-Economic Analysis of Alcohol-to-Jet Fuel Production.” *Biotechnology for Biofuels*, Vol. 10, No. 1, 2017, p. 18. <https://doi.org/10.1186/s13068-017-0702-7>.
- [72] Shapouri, H., and Salassi, M. *The Economic Feasibility of Ethanol Production From Sugar in the United States*. USDA, 2006.
- [73] Niziolek, A. M., Onel, O., Hasan, M. M. F., and Floudas, C. A. “Municipal Solid Waste to Liquid Transportation Fuels – Part II: Process Synthesis and Global Optimization Strategies.” *Computers & Chemical Engineering*, Vol. 74, 2015, pp. 184–203. <https://doi.org/10.1016/j.compchemeng.2014.10.007>.
- [74] Hans Kandel. “Canola Production Field Guide.” *NDSU Extension Service*, 2011.
- [75] E.S. Oplinger, L.L. Hardman, E.T. Gritton, J.D. Doll, and K.A. Kelling. Canola (Rapeseed). <https://hort.purdue.edu/newcrop/afcm/canola.html>. Accessed May 24, 2021.

- [76] Texas Crop and Livestock Budgets. *Texas A&M AgriLife Extension*. <https://agecoext.tamu.edu/resources/crop-livestock-budgets/>. Accessed May 24, 2021.
- [77] 2021 Farm Management Guides for Non-Irrigated Crops. *Kansas State University AgManager*. <https://agmanager.info/farm-budgets/2021-farm-management-guides-non-irrigated-crops>. Accessed May 24, 2021.
- [78] Budgets — Farm Management. *North Dakota State University*. <https://www.ag.ndsu.edu/farmmanagement/crop-budget-archive>. Accessed May 24, 2021.
- [79] Arkansas Field Crop Enterprise Budgets. *University of Arkansas Division of Agriculture*. <https://www.uaex.uada.edu/farm-ranch/economics-marketing/farm-planning/budgets/crop-budgets.aspx>. Accessed May 24, 2021.
- [80] Crop Budgets. *University of Maryland Extension*. <https://extension.umd.edu/programs/agriculture-food-systems/program-areas/farm-and-agribusiness-management/grain-marketing/crop-budgets>. Accessed May 24, 2021.
- [81] Budgets. *College of Agricultural and Environmental Sciences: University of Georgia*. <https://agecon.uga.edu/extension/budgets.html>. Accessed May 24, 2021.
- [82] Nebraska Crop Budgets. *University of Nebraska - Lincoln*. <https://cropwatch.unl.edu/budgets>. Accessed May 24, 2021.
- [83] Enterprise Budgets. *NC State University*. <https://cals.ncsu.edu/are-extension/business-planning-and-operations/enterprise-budgets/>. Accessed May 24, 2021.
- [84] Budgets. Department of Agricultural and Resource Economics: UT Institute of Agriculture, Sep 19, 2020.
- [85] Missouri Crop and Livestock Enterprise Budgets. *MU Extension*. <https://extension.missouri.edu/programs/agricultural-business-and-policy-extension/missouri-crop-and-livestock-enterprise-budgets>. Accessed May 24, 2021.
- [86] Enterprise Budgets - Crop. *Colorado State University Extension*. <https://abm.extension.colostate.edu/enterprise-budgets-crop/>. Accessed May 24, 2021.
- [87] Budgets. *Agricultural Economics | Mississippi State University*. <http://www.agecon.msstate.edu/whatwedo/budgets.php>. Accessed May 24, 2021.
- [88] Enterprise Budgets for Row Crops. *Alabama Cooperative Extension System*. <https://www.aces.edu/blog/topics/farm-management/enterprise-budgets-for-row-crops/>. Accessed May 24, 2021.
- [89] Budgets and Decision Tools. *University of Kentucky Agricultural Economics*. <https://agecon.ca.uky.edu/budgets>. Accessed May 24, 2021.
- [90] Budgets. *LSU AgCenter*. https://www.lsuagcenter.com/portals/our_offices/departments/ag-economics-agribusiness/extension_outreach/budgets. Accessed May 24, 2021.
- [91] 2021 Purdue Crop Cost & Return Guide. https://ag.purdue.edu/commercialag/home/wp-content/uploads/2020/03/id-166_2021-october-2020-projections.pdf. Accessed May 24, 2021.
- [92] Crop Budgets. *University of Idaho*. <https://www.uidaho.edu/cals/idaho-agbiz/crop-budgets>. Accessed May 24, 2021.
- [93] Current Cost and Return Studies. *Agricultural & Resource Economics | UC Davis*. <https://coststudies.ucdavis.edu/en/current/>. Accessed May 24, 2021.
- [94] Crop Budgets. *University of Minnesota Extension*. <https://extension.umn.edu/farm-finance/crop-budgets>. Accessed May 24, 2021.
- [95] Jack Davis. Crop Budgets. *South Dakota State University Extension*. <https://extension.sdstate.edu/crop-budgets>. Accessed May 24, 2021.
- [96] Ohio Crop Enterprise Budgets. *Ohio State University Extension*. <https://farmoffice.osu.edu/blog-tags/ohio-crop-enterprise-budgets>. Accessed May 24, 2021.
- [97] Khanna, M., Dhungana, B., and Clifton-Brown, J. “Costs of Producing Miscanthus and Switchgrass for Bioenergy in Illinois.” *Biomass and Bioenergy*, Vol. 32, No. 6, 2008, pp. 482–493. <https://doi.org/10.1016/j.biombioe.2007.11.003>.

- [98] Mainul Hoque, Georgeanne Artz, and Chad Hart. Estimated Cost of Establishment and Production of Miscanthus in Iowa. <https://www.extension.iastate.edu/agdm/crops/pdf/a1-28.pdf>. Accessed May 24, 2021.
- [99] Michael Jacobson. Miscanthus Budget for Biomass Production. *Penn State Extension*. <https://extension.psu.edu/miscanthus-budget-for-biomass-production>. Accessed May 24, 2021.
- [100] Crop Enterprise Budget: Irrigated Sugarbeet, Goshen County Wyoming. <http://wyoextension.org/publications/html/B1315-4/>. Accessed May 24, 2021.
- [101] Haque, M., Epplin, F., and Taliaferro, C. “Nitrogen and Harvest Frequency Effect on Yield and Cost for Four Perennial Grasses.” *undefined*, 2009.
- [102] Bonnie Ownley, Ken Goddard, G. Neil Rhodes Jr., Don Tyler, and Jon Walton. Guidebook for the Sustainable Production Practices of Switchgrass in the Southeastern U.S. *Southeastern Partnership for Integrated Biomass Supply Systems*. <http://www.se-ibss.org/publications-and-patents/extension-and-outreach-publications/guidebook-for-the-sustainable-production-practices-of-switchgrass-in-the-southeastern-u.s>. Accessed May 24, 2021.
- [103] Wang, M., Han, J., Dunn, J. B., Cai, H., and Elgowainy, A. “Well-to-Wheels Energy Use and Greenhouse Gas Emissions of Ethanol from Corn, Sugarcane and Cellulosic Biomass for US Use.” *Environmental Research Letters*, Vol. 7, No. 4, 2012, p. 045905. <https://doi.org/10.1088/1748-9326/7/4/045905>.
- [104] Cai, H., Dunn, J. B., Wang, Z., Han, J., and Wang, M. Q. “Life-Cycle Energy Use and Greenhouse Gas Emissions of Production of Bioethanol from Sorghum in the United States.” *Biotechnology for Biofuels*, Vol. 6, No. 1, 2013, p. 141. <https://doi.org/10.1186/1754-6834-6-141>.
- [105] Ali, M. B. “Characteristics and Production Costs of U.S. Wheat Farms.” 2002, p. 44.
- [106] European Commission. Joint Research Centre. *Definition of Input Data to Assess GHG Default Emissions from Biofuels in EU Legislation :Version 1d 2019*. Publications Office, LU, 2019.
- [107] Ali, M. “Characteristics and Production Costs of U.S. Sugarbeet Farms.” 2004, p. 42.
- [108] Han, J., Elgowainy, A., Dunn, J. B., and Wang, M. Q. “Life Cycle Analysis of Fuel Production from Fast Pyrolysis of Biomass.” *Bioresource Technology*, Vol. 133, 2013, pp. 421–428. <https://doi.org/10.1016/j.biortech.2013.01.141>.
- [109] Deliberto, M. A., and Hilbun, B. M. “PROJECTED COSTS AND RETURNS CROP ENTERPRISE BUDGETS FOR CORN PRODUCTION IN LOUISIANA, 2021.” p. 46.
- [110] Davis, R. E., Grundl, N. J., Tao, L., Bidy, M. J., Tan, E. C., Beckham, G. T., Humbird, D., Thompson, D. N., and Roni, M. S. *Process Design and Economics for the Conversion of Lignocellulosic Biomass to Hydrocarbon Fuels and Coproducts: 2018 Biochemical Design Case Update; Biochemical Deconstruction and Conversion of Biomass to Fuels and Products via Integrated Biorefinery Pathways*. Publication NREL/TP--5100-71949, 1483234. 2018, p. NREL/TP--5100-71949, 1483234.
- [111] Geleynse, S., Brandt, K., Garcia-Perez, M., Wolcott, M., and Zhang, X. “The Alcohol-to-Jet Conversion Pathway for Drop-In Biofuels: Techno-Economic Evaluation.” *ChemSusChem*, Vol. 11, No. 21, 2018, pp. 3728–3741. <https://doi.org/10.1002/cssc.201801690>.
- [112] Yusuf, A., Giwa, A., Mohammed, E. O., Mohammed, O., Al Hajaj, A., and Abu-Zahra, M. R. M. “CO₂ Utilization from Power Plant: A Comparative Techno-Economic Assessment of Soda Ash Production and Scrubbing by Monoethanolamine.” *Journal of Cleaner Production*, Vol. 237, 2019, p. 117760. <https://doi.org/10.1016/j.jclepro.2019.117760>.
- [113] Davis, R., Tao, L., Scarlata, C., Tan, E. C. D., Ross, J., Lukas, J., and Sexton, D. *Process Design and Economics for the Conversion of Lignocellulosic Biomass to Hydrocarbons: Dilute-Acid and Enzymatic Deconstruction of Biomass to Sugars and Catalytic Conversion of Sugars to Hydrocarbons*. Publication NREL/TP--5100-62498, 1176746. 2015, p. NREL/TP--5100-62498, 1176746.
- [114] Swanson, R. M., Platon, A., Satrio, J. A., Brown, R. C., and Hsu, D. D. *Techno-Economic Analysis of Biofuels Production Based on Gasification*. Publication NREL/TP-6A20-46587, 994017. 2010, p. NREL/TP-6A20-46587, 994017.